

AD-A144 282

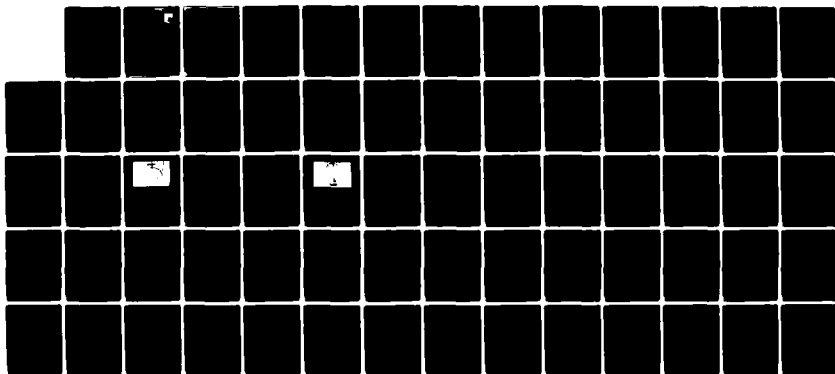
PULSED INDUCTIVE ENERGY STORE(U) IAP RESEARCH INC
DAYTON OH D E JOHNSON ET AL. MAY 84 IAP-TR-83-5
AFWAL-TR-84-2031 F33615-82-C-2224

1.1

UNCLASSIFIED

F/G 10/2

NL



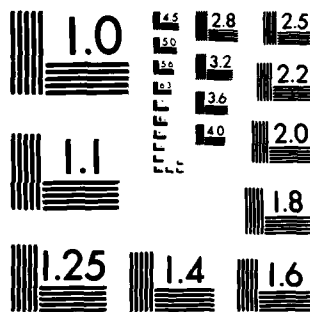
END

DATE

FILED

9 84

DTIC



MICROCOPY RESOLUTION TEST CHART
NATIONAL BUREAU OF STANDARDS-1963-A

AFVAL-TR-84-2031

PULSED INDUCTIVE ENERGY STORE



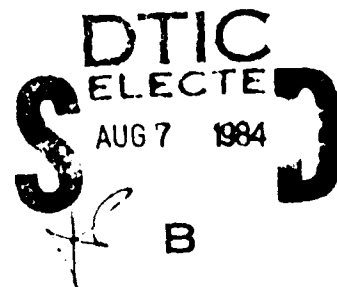
AD-A144 282

IAP RESEARCH, INC.
7546 MCEWEN RD.
DAYTON, OHIO 45459

MAY 1984

FINAL REPORT FOR PERIOD JULY 1982 - JANUARY 1984

APPROVED FOR PUBLIC RELEASE; DISTRIBUTION UNLIMITED



AERO PROPULSION LABORATORY
AIR FORCE WRIGHT AERONAUTICAL LABORATORIES
AIR FORCE SYSTEMS COMMAND
WRIGHT PATTERSON AIR FORCE BASE, OHIO 45433

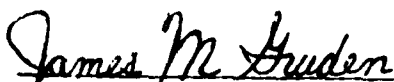
84 08 07 068

NOTICE

When government drawings, specifications, or other data are used for any purpose other than in connection with a definitely related Government procurement operation, the United States Government thereby incurs no responsibility nor any obligation whatsoever and the fact that the government may have formulated, furnished, or in any way supplied the said drawings, specifications, or other data, is not to be regarded by implication or otherwise as in any manner licensing the holder or any other person or corporation, or conveying any rights or permission to manufacture use, or sell any patented invention that may in any way be related thereto.

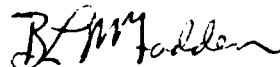
This report has been reviewed by the Office of Public Affairs (ASD/PA) and is releasable to the National Technical Information Service (NTIS). At NTIS, it will be available to the general public, including foreign nations.

This technical report has been reviewed and is approved for publication.



JAMES M. GRUDEN, 1LT, USAF
Power Systems Branch
Aerospace Power Division
Aero Propulsion Laboratory

FOR THE COMMANDER



B. L. MCFADDEN, Acting Chief
Power Systems Branch
Aerospace Power Division
Aero Propulsion Laboratory



JAMES D. REAMS
Chief, Power Systems Branch
Aerospace Power Division
Aero Propulsion Laboratory

'If your address has changed, if you wish to be removed from our mailing list, or if the addressee is no longer employed by your organization please notify AFVAL/POOS-2, WPAFB, OH 45433 to help us maintain a current mailing list.'

Copies of this report should not be returned unless return is required by security considerations, contractual obligations, or notice on a specific document.

Unclassified

SECURITY CLASSIFICATION OF THIS PAGE (When Data Entered)

REPORT DOCUMENTATION PAGE		READ INSTRUCTIONS BEFORE COMPLETING FORM	
1. REPORT NUMBER AFWAL-TR-84-2031	2. GOVT ACCESSION NO. A144282	3. RECIPIENT'S CATALOG NUMBER	
4. TITLE (and Subtitle) PULSED INDUCTIVE ENERGY STORE		5. TYPE OF REPORT & PERIOD COVERED Final Report July 1982 - January 1984	
7. AUTHOR(s) Donald E. Johnson John P. Barber		6. PERFORMING ORG. REPORT NUMBER IAP-TR-83-5	
9. PERFORMING ORGANIZATION NAME AND ADDRESS IAP Research, Inc. 7546 McEwen Rd. Dayton, Ohio 45459		8. CONTRACT OR GRANT NUMBER(s) F33615-82-C-2224	
11. CONTROLLING OFFICE NAME AND ADDRESS Aero Propulsion Laboratory (AFWAL/POOS) Air Force Wright Aeronautical Laboratories (AFSC) Wright-Patterson AFB, Ohio 45433		10. PROGRAM ELEMENT, PROJECT, TASK AREA & WORK UNIT NUMBERS	
14. MONITORING AGENCY NAME & ADDRESS (if different from Controlling Office)		12. REPORT DATE May 1984	
		13. NUMBER OF PAGES 61	
		15. SECURITY CLASS. (of this report) Unclassified	
		15a. DECLASSIFICATION/DOWNGRADING SCHEDULE	
16. DISTRIBUTION STATEMENT (of this Report) Approved for public release; distribution unlimited.			
17. DISTRIBUTION STATEMENT (of the abstract entered in Block 20, if different from Report)			
18. SUPPLEMENTARY NOTES			
19. KEY WORDS (Continue on reverse side if necessary and identify by block number) High Current Inductor - Toroidal			
20. ABSTRACT (Continue on reverse side if necessary and identify by block number) The objective of this program was to evaluate the technical feasibility of coaxial toroidal coils as high current pulsed energy storage inductors. The program included an analytic investigation, and the design, fabrication and testing of a cryogenically cooled coaxial toroidal coil. The most promising concept we investigated was a multiturn sector inductor constructed by arranging several pancake coils (sectors) so that they approximate a toroid and connecting the coils electrically in parallel. The advantage of the sector inductor concept is that coil construction is considerably (over)			

DD FORM 1 JAN 73 1473 EDITION OF 1 NOV 65 IS OBSOLETE

UNCLASSIFIED

SECURITY CLASSIFICATION OF THIS PAGE (When Data Entered)

Unclassified

SECURITY CLASSIFICATION OF THIS PAGE(When Data Entered)

20 Cont'd.

simpler than with other toroidal designs. We modeled the sector coil on a computer and calculated the magnitude of the fringing fields for coils of various numbers of sectors. We designed, fabricated, and tested a 10 kA demonstration coil. The performance of the demonstration coil surpassed all design parameters. The coil conducted peak currents of 9.2 kA and pulses of 5 kA for up to 8.9s. Testing was limited by the maximum current available at the test facility. We were not able to detect a significant increase in resistance during any of the tests. To verify current sharing among sectors, we measured individual sector currents at various coil currents. Four sectors conducted within 1.5% of one sixth of the total coil current. One sector conducted 6.4% more than one sixth and another conducted 5.3% less than one sixth of the total coil current.

Unclassified

SECURITY CLASSIFICATION OF THIS PAGE(When Data Entered)

TABLE OF CONTENTS

Section		Page
1	INTRODUCTION	1
2	HIGH CURRENT INDUCTIVE ENERGY STORAGE	2
2.1	Cryogenic Coils	2
2.2	Multiturn Inductors	5
2.3	Toroidal Inductors	6
2.4	The Multiturn Sectored Inductor	7
3	SECTORED COIL DESIGN	9
3.1	Fringing Fields	9
3.1.1	Fringing Field Analysis	9
3.1.1.1	Theory	9
3.1.1.2	Computer Modeling	10
3.1.1.3	Description of the Coil Geometry	11
3.1.2	Summary of the Fringing Fields Study	12
3.2	Sizing	12
3.2.1	Inductance	13
3.2.2	Stress Constraint Effects	14
3.2.3	Thermal Constraints	16
3.2.4	Resistance	16
3.2.5	High Frequency Constraints	16
3.2.5.1	High Frequency Effect on Inductance	16
3.2.5.2	High Frequency Effect on Resistance	18
4	THE DEMONSTRATION COIL	19
4.1	Demonstration Coil Parameters	19
4.2	Forced Cooling System	20
4.3	Testing	22
4.3.1	Impedance Measurements	22
4.3.1.1	Inductance	23
4.3.1.2	Resistance	28
4.3.2	Current Tests	30
4.3.2.1	Terminal Characteristics -- Resistance	30
4.3.2.2	Current Sharing	32
4.3.3	Forced Cooling System	34
4.4	Evaluation	34
4.4.1	Coil Resistance	35
4.4.2	Current Sharing	35
4.4.3	Forced Convective Cooling	36
5	CONCLUSIONS	37
6	RECOMMENDATIONS	38
A	MAGNETIC FRINGING FIELDS AROUND A MULTISECTOR TOROIDAL INDUCTOR	39
B	RESEARCH AND DEVELOPMENT TEST PLAN FOR THE PULSED INDUCTIVE ENERGY STORE	52

LIST OF FIGURES

Figure		Page
1	Resistivity of Aluminum As a Function of Temperature	3
2	Power Requirements for an Electromagnetic Gun System with Cryogenically Cooled Aluminum Coils	4
3	Electromagnetic Gun System Mass with Cryogenically Cooled Aluminum Coils	5
4	A Coaxial Toroidal Inductor	6
5	A Sected Coaxial Toroid	7
6	The Magnetic Field at a Point Due to a Filamentary Current, i , Can Be Calculated Using the Biot-Savart Law	10
7	A Four-Sector Filamentary Coaxial Coil	11
8	A Circular Toroid	14
9	A D-Shaped Toroid	15
10	A Rectangular Toroid	15
11	Flux Trapping in a Solenoidal Coil	17
12	The Demonstration Coil Concept	19
13	Coolant Flow to the Demonstration Coil	21
14	Coolant Flows from the Core Region Out Between Sectors, Cooling the Edges of the Conductors	21
15	The Coolant Supply Pipe, Core Region, and Coolant Channels are Visible in This View of the Partially Assembled Coil.	22
16	Shorting Strips Replace the Coil Sectors During a Down-Lead Impedance Measurement.	25
17	Three Mutually Coupled Inductors in Parallel	27
18	The Coupling Coefficient Versus Angle Between Two Sectors	27
19	Inductance of the Coil Components Versus Frequency	28
20	A Terminal Measurement Technique	30
21	Coil Voltage Versus Current at Constant Resistance	32

LIST OF TABLES

Table		Page
1	Demonstration Coil Characteristics	20
2	Series and Parallel Impedance of Coil Sectors	24
3	Series and Parallel Impedance of Coil Sectors After Cleaning Process	24
4	Inductance of Partial Coil Assemblies	26
5	Resistivity of 1100-0 Aluminum at Room Temperature and Boiling Nitrogen Temperature	29
6	Impedance of the Pulsed Energy Storage Coil at Room Temperature and Boiling Nitrogen Temperature	29
7	Coil Resistance for Various Current Pulses	33
8	Sector Current at Seven Test Current Levels	34

Accession For	
NTIS GEAR1	<input checked="" type="checkbox"/>
DTIC TAB	<input type="checkbox"/>
Unannounced	<input type="checkbox"/>
Justification	
By	
Distribution/	
Availability Codes	
Dist	Avail and/or Special
A-1	



SECTION 1

INTRODUCTION

Recent developments in pulsed power applications have created a pressing need for improved pulsed energy storage coils. New applications such as electromagnetic launchers and propulsion systems typically require low-inductance, high-current energy stores. A typical energy store might be tens of microhenries capable of conducting peak currents of hundreds of kiloamperes. As practical pulsed power applications (as opposed to laboratory experiments) are envisioned, there is a substantial premium on compact, low-mass, low-resistance designs. A third constraint imposed by practical applications is that electromagnetic interference caused by the storage coil must be reduced to tolerable levels. This combination of requirements is extremely demanding and there are no proven coil designs which entirely satisfy these needs. The purpose of this program was to investigate an advanced coil design which showed promise of meeting these new pulsed power requirements.

The remainder of this report is divided into five major sections and two appendixes. In Section 2 we address the general concepts of inductive energy storage and introduce the multiturn sectorized inductor. We describe the design elements that are particular to the sectorized toroidal coil in Section 3. Section 4 is devoted to the 10,000 A demonstration coil that was designed, constructed, and tested. Our conclusions and recommendations are listed in Sections 5 and 6 respectively. A fringing field analysis of coaxial sectorized coils is included as Appendix A. Finally, the demonstration coil research and development test plan is presented as Appendix B.

SECTION 2

HIGH CURRENT INDUCTIVE ENERGY STORAGE

A number of important design constraints must be considered for an energy storage coil in a high-current pulsed power application such as an electromagnetic gun. These constraints include resistive losses, coil mass, external fringing fields, and mechanical integrity. Coil resistive losses directly affect overall system efficiency and reflect directly to power system and fuel mass. It is therefore desirable to reduce resistive losses to the lowest practical value. The inductive energy storage coil is often a significant part of system mass and the mass of the coil itself is therefore an important design parameter. Mass and resistance must inevitably be traded off to arrive at an optimum design which minimizes total system mass. The fringing or external fields produced by the energy storage coil can have significant and detrimental effects on other parts of the system and on other systems which must operate close to the coil (e.g., aircraft avionics). It is therefore highly desirable, and may be essential, to design energy storage coils with zero or very small external fields. Finally, the high current applications now being considered (such as railguns) impose very high mechanical loads on the coil conductors. These mechanical loads play an important, and often critical part, in coil design. The discussion in the following sections deals with some of the common tradeoffs in practical coil design.

2.1 CRYOGENIC COILS

Two principal constraints on practical coils are resistance and mass. The resistance of a coil may be expressed as

$$R = \eta l / A \quad (1)$$

where η = material resistivity
 l = length of conductor
 A = cross-sectional area of conductor.

The length of the conductor is determined by the inductance required and is not free to be chosen to minimize resistance. Resistance may therefore be

minimized by decreasing the material resistivity and/or increasing the conductor cross-sectional area. The mass of conductor in the coil is given by

$$M = \rho l A \quad (2)$$

where ρ = conductor density.

From Equation 2 we see that increasing the cross-sectional area in order to decrease resistance has the counterproductive effect of increasing conductor mass. We are therefore left with the task of reducing material resistivity.

One method of reducing the resistivity of a material is to cool it to cryogenic temperatures. The resistivity of aluminum as a function of temperature is illustrated in Figure 1. The resistivity is observed to decrease by more than three orders of magnitude from room temperature to liquid hydrogen temperatures. While commercial purity aluminum (>99.5% Al)

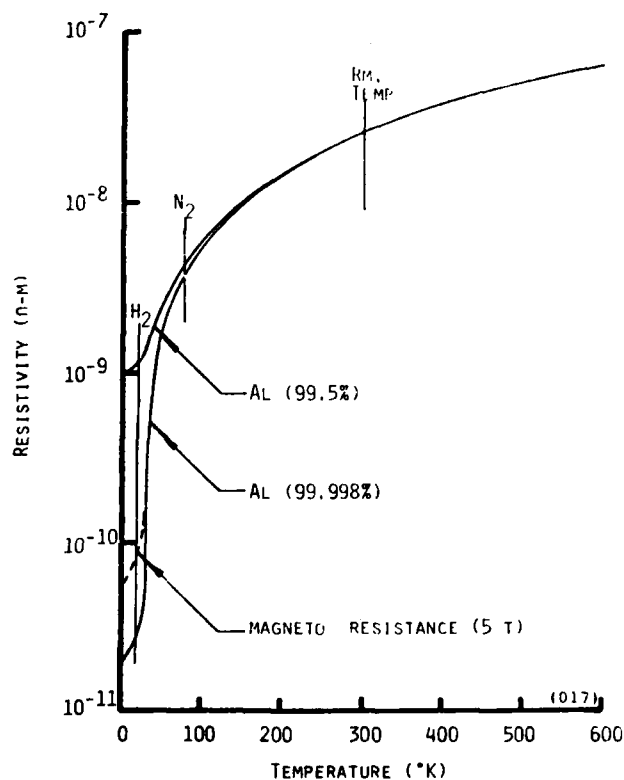


Figure 1. Resistivity of Aluminum As a Function of Temperature.

does not exhibit the same dramatic decrease in resistance at liquid hydrogen temperatures, its resistivity does decrease by typically seven times from room temperature to liquid nitrogen temperature.

In order to assess the potential impact of the use of cryogenically cooled aluminum coils on electromagnetic gun system performance, we conducted a preliminary assessment using our existing electromagnetic gun system model. The power requirements for a rapid fire system are illustrated in Figure 2. An aluminum coil operated at room temperature resistively dissipates approximately one third of the system power. By operating a high purity aluminum coil at liquid nitrogen temperature, coil losses can be reduced to approximately 5% of losses at room temperature.

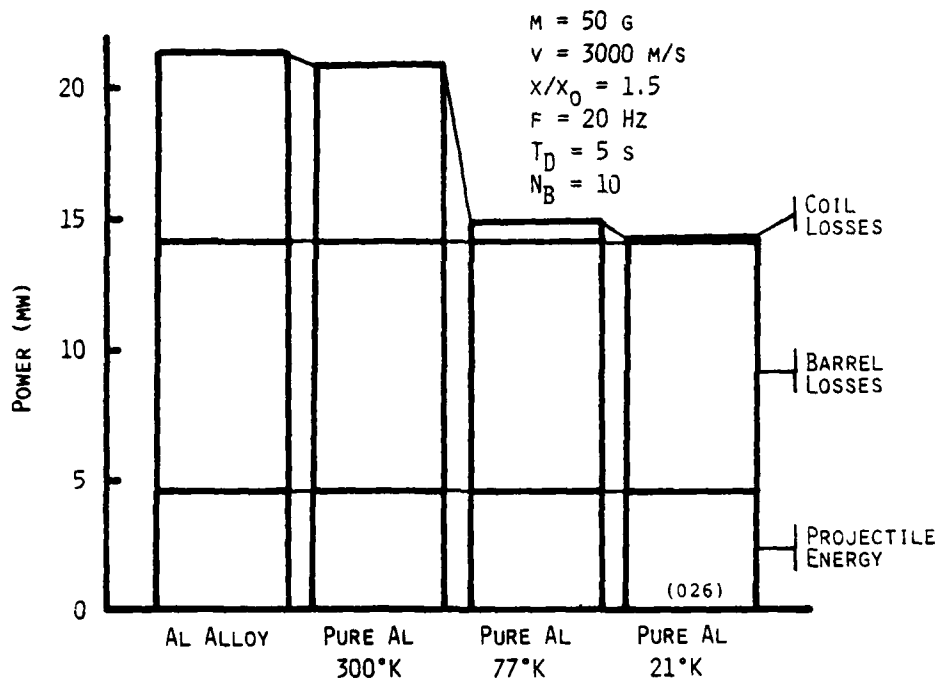


Figure 2. Power Requirements for an Electromagnetic Gun System with Cryogenically Cooled Aluminum Coils.

The reduced power requirements illustrated in Figure 2 imply significant savings in overall system mass. System mass variations are illustrated in Figure 3. The increased efficiency obtainable with cryogenic coils may result in a significant reduction in overall system mass, particularly in fuel requirements. The use of cryogenically cooled aluminum coils for high-current pulsed energy storage is clearly attractive.

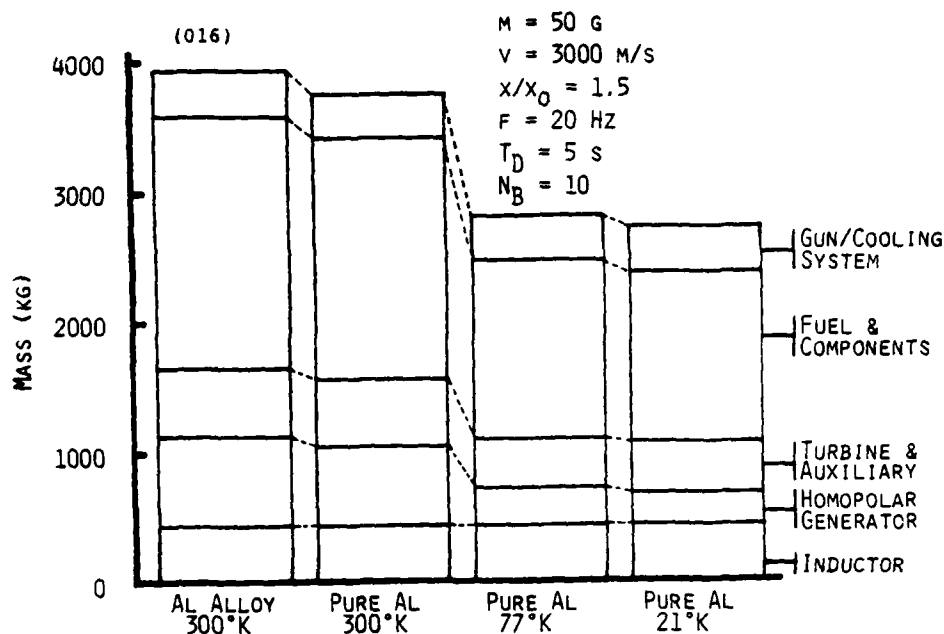


Figure 3. Electromagnetic Gun System Mass with Cryogenically Cooled Aluminum Coils.

2.2 MULTITURN INDUCTORS

The choice of inductor geometry is strongly influenced by a practical design application. Of the four simple classes of coil configuration, parallel plate and coaxial transmission lines represent the simplest mechanical configurations. A parallel plate transmission line is unsuitable because of the relatively high external magnetic field which it produces. A coaxial transmission line, on the other hand, has zero external field and is extremely robust mechanically (there are no unbalanced forces). A coaxial transmission line unfortunately has a very low inductance per unit mass. In fact, the inductance per unit mass of any single turn device (such as a transmission line) is unattractive when compared with that of a multi-turn device (such as a solenoid or toroid).

Both solenoids and toroids can have very high inductance per unit mass due to the flux linkage between turns. The inductance per unit mass varies approximately as $1/n$ where n is the number of turns. Solenoids in general produce high external fields and are therefore unsuitable for many high-current pulse power applications. Toroids produce very low external fields, so we shall restrict our attention to toroidal multiturn configurations.

2.3 TOROIDAL INDUCTORS

The chief disadvantage of toroidal coils is that they are difficult to construct with conductors capable of conducting very high currents. Construction problems are intensified when multi-turn designs are envisioned. Several toroidal inductors have been constructed by first winding a solenoid, and then bending the ends around until they meet, forming a right circular torus. This technique cannot be considered for multi-hundred kiloampere coils. The conductors would generally be so large that 'bending the ends around' would be nearly impossible.

One manner in which a toroidal coil might be realized is the 'coaxial' coil geometry shown in Figure 4. The coil is considered coaxial because each turn can be thought of as a section of electrically shorted coaxial cable. The coaxial coil as shown is still difficult to realize physically. Joining of the tubes to the end plates while preserving inter-turn insulation would require intricate construction methods. We also concluded that it would be prohibitively difficult to use high purity materials in the tube and end plate design. The difficulty occurs because it is nearly impossible

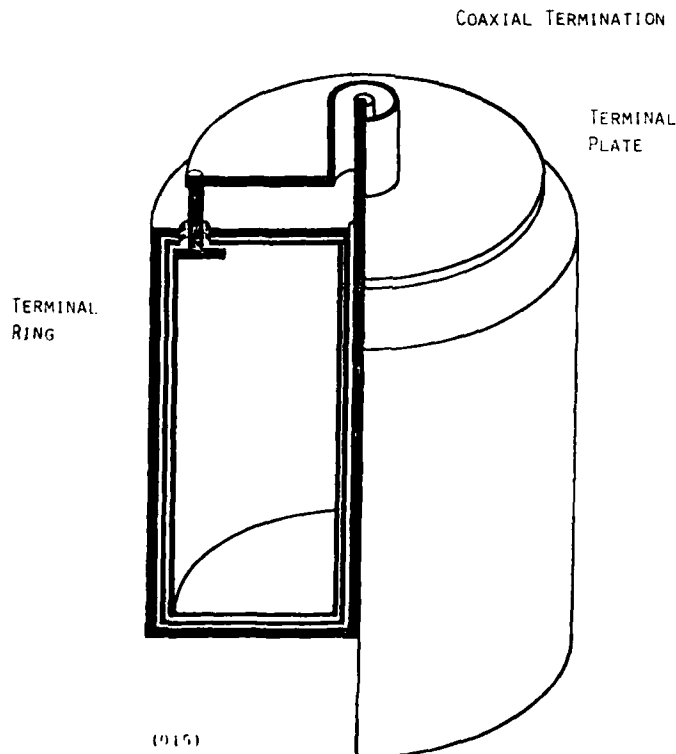


Figure 4. A Coaxial Toroidal Inductor.

to join high purity materials while retaining low resistivity at low cryogenic temperatures. An approach which may solve the construction problem of coaxial toroidal coils, while preserving the advantages of low leakage fields, is the 'sectored' coaxial coil described in the following section.

2.4 THE MULTITURN SECTORED INDUCTOR

The concept of a multiturn sectored inductor is depicted in Figure 5. The symmetrical arrangement of return paths around a central core approximates the closed coaxial toroid shown in Figure 4 and thus preserves the characteristic low value of leakage flux. The advantage of the sectored concept is that coil construction is considerably simpler than with other toroidal designs.

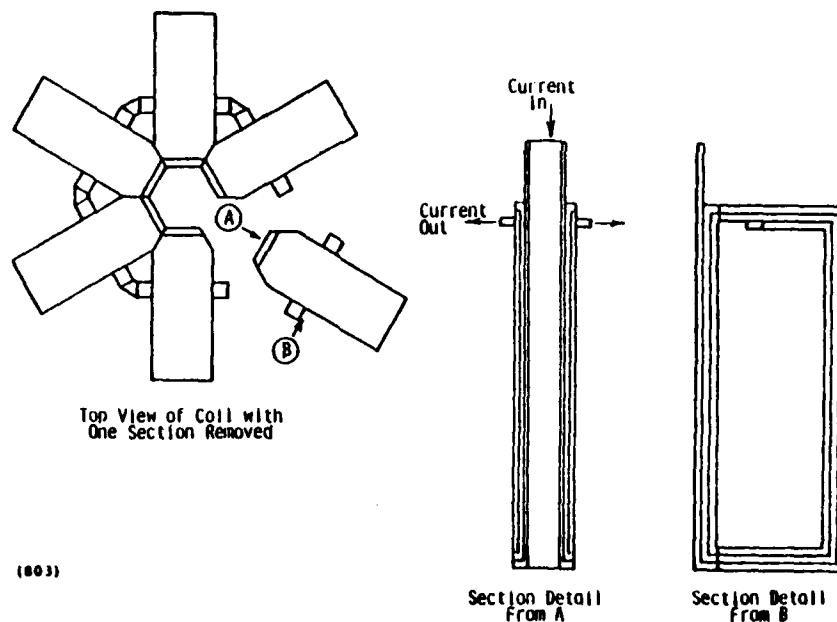


Figure 5. A Sektored Coaxial Toroid.

In the sectored concept the toroid is constructed in segments. Each segment is fabricated separately as a 'pancake' coil. The core area of each pancake coil is milled into a wedge shape and the segments are assembled in the 'sectored' configuration. Electrically and mechanically, the core region is nearly coaxial. Fabrication by this technique is

relatively straightforward. The pancake coil configuration has been used extensively in high-field magnet design and is the primary concept used for high purity aluminum coils. The cross-section of the toroid can be nearly any desired shape. All that is required to define the cross-section of the toroid is to wind the pancake coils on a mandrel having the same shape as the desired cross-section of the toroid.

A possible disadvantage of building a sectored coil rather than a completely enclosed toroid is the presence of fringing fields. The return conductors in the toroid do not entirely close the toroid in. More complete closure, which would result in smaller fringing fields, can be achieved by increasing the number of sectors. An important design point for a practical coil would be the number of sectors needed to reduce the fringing fields to acceptable levels for nearby electronics. A sectored toroidal coil represents a class of practical coil designs that offers high current capacity, low mass, and minimal external fields.

SECTION 3

SECTORED COIL DESIGN

The design of a sectored toroidal coil shares many of the same aspects as the design of more conventional coils. In this section we will discuss both the unique aspects of sectored coils and the common aspects of inductive energy stores. The first design step is unique to sectored toroidal inductors: one must determine the number of sectors needed to approximate a closed toroid and thus reduce the magnitude of fringing fields to an acceptable level. The other design points can be broadly characterized together as 'sizing' and are common to the design of all types of inductive energy stores. Sizing consists of designing a coil to have the required inductance and resistance, while meeting the allowable stress and thermal constraints of the coil structure. The following sections describe the details of selecting and sizing a sectored toroidal coil.

3.1 FRINGING FIELDS

The magnitude of the leakage fields is inversely proportional to the number of symmetric return paths or 'sectors' used. That is, the more sectors that are used, the better the shielding will be. Unfortunately, the construction may be more difficult with greater numbers of sectors. The design problem is then to determine how many sectors provides 'adequate' shielding, and more exactly, how the number of sectors relates to the magnitude of the fringing fields.

3.1.1 Fringing Field Analysis

The emphasis of the fringing field investigation was to find a relationship between the number of coil sectors and the magnitude of fringing fields. During the study, areas of high and low field magnitude around the coil were defined. These definitions could aid in orienting the coil to avoid interference with sensitive electronic equipment.

3.1.1.1 Theory

The magnetic field that occurs at a point, due to the flow of current in a flat strip, can be approximated by current flowing in a linear fila-

ment, as long as the point is an appreciable distance away from the conductor. An appreciable distance would be 2 to 3 conductor widths for a strip whose length is much greater than its width. The magnetic field due to a filamentary current, such as that shown in Figure 6, can be calculated using the Biot-Savart Law:

$$dB = (\mu_0 i d\ell \sin\theta) / 4\pi r^2 \quad (3)$$

where B = magnetic flux density,

μ_0 = permeability of free space,

i = filamentary current,

$d\ell$ = length of the filament, and

θ = angle between the $d\ell$ vector and a vector directed from the midpoint of $d\ell$ to P , the point at which the field is evaluated.

The expression for dB can be integrated to find the field due to a finite length of conductor or a group of such conductors.

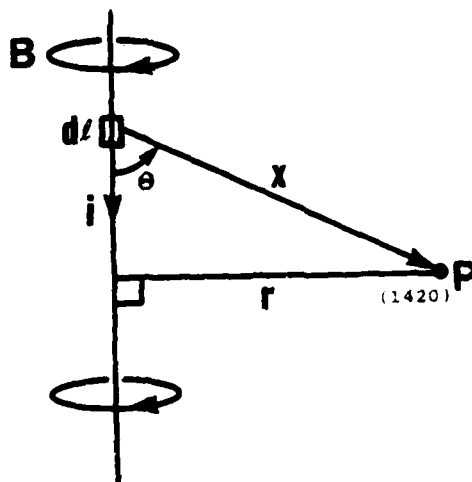
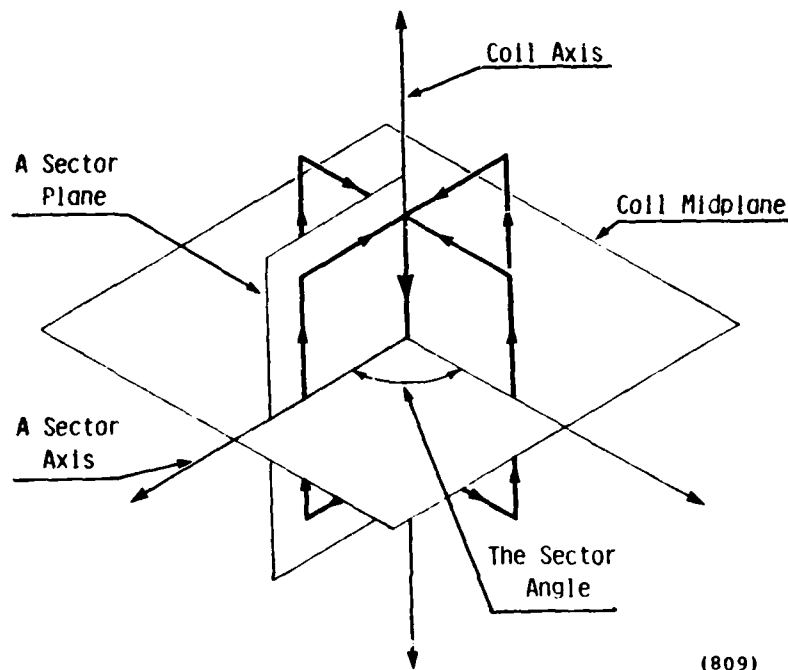


Figure 6. The Magnetic Field at a Point Due to a Filamentary Current, i , Can Be Calculated Using the Biot-Savart Law.

3.1.1.2 Computer Modeling

We used a digital computer to integrate Equation 3 and evaluate the magnetic field at various points around filamentary inductors composed of N_s sectors. A schematic of such a filamentary inductor with 4 sectors ($N_s = 4$) is shown in Figure 7. Regions of high and low field intensity were



(809)

Figure 7. A Four-Sector Filamentary Coaxial Coil.

identified and finally, a curve fitting routine was used to define the relationship of the magnitude of the field to the number of sectors in the highest field region.

3.1.1.3 Description of the Coil Geometry

In order to describe the fields around an inductor, it is necessary to define several terms relating to the coil geometry. Referring to Figure 7, the following terms are defined:

- coil axis - defined in the usual manner for toroids, as illustrated
- coil midplane - the plane bisecting the toroid and normal to the coil axis
- coil center - the intersection of the coil axis and the coil midplane
- sector - a single section of the coil
- sector plane - the plane of a sector
- sector axis - the axis originating at the coil center and extending along the intersection of the sector plane and the coil midplane
- coil radius - a , the dimension of a sector along the sector axis

- r - the distance from the coil center normalized to the coil radius ($r = R/a$, where R is the absolute distance from the coil center to the point of interest)

3.1.2 Summary of the Fringing Fields Study

A detailed report of the fringing field analysis is appended to this report. The results of the field analysis in the region surrounding a sectorized toroidal coil can be summarized as:

1. The magnitude of the magnetic field is greatest along the sector axis and lowest near the coil axis.
2. The magnitude of the field directly on the coil axis is zero.
3. The magnitude of the field at a fixed point on the sector axis varies as approximately one over the number of coil sectors. For more than three sectors, this is a relatively weak dependence.
4. The magnitude of the fringing fields along the sector axis decreases as about $1/r^8$ for a six sector-coil.
5. The choice of the number of sectors is only critical when system design requires that sensitive equipment be placed close to the coil. Orientation of the coil and distance to the sensitive equipment will usually have a greater effect on fringing fields than the number of sectors.

3.2 SIZING

The first consideration in sizing and designing a coil is the inductance. The inductance is usually specified by the application. That is, the designer is not free to choose the inductance, but must design the coil to have the inductance required by the application. However, given an inductance value, there is an infinite set of possible inductor configurations and sizes which will provide the required inductance. The designer's task is to choose the coil configuration and size best suited to the application.

For most applications of Air Force interest, minimizing inductor mass is the primary design goal. Additional design goals might include minimization of external or fringing fields and minimization of coil volume. As this discussion progresses we shall examine the impact of these other factors. However, the primary optimization goal, we believe, is to minimize coil mass. We now examine the implications of this goal.

3.2.1 Inductance

The inductance of any coil can be written as

$$L_o = k l N \quad (4)$$

where l = length of conductor

N = number of turns

k = coil factor which depends only on coil configuration, not on coil size.

The mass of a coil can be written approximately as

$$m \approx \rho l A \quad (5)$$

where ρ = density of conductors

A = cross-sectional area of conductors.

Combining Equations 4 and 5 we obtain

$$m = \rho A L_o / k N \quad (6)$$

L_o is fixed by the application (i.e., it cannot be varied to minimize mass). The conductor density, ρ , is fixed by the choice of conductor material. As we shall see later, the choice of conductor material is constrained by other factors and the conductor density is not necessarily free to be chosen to minimize mass. Inspection of Equation 6 shows that design, therefore, must concentrate on minimizing conductor cross-sectional area, A ; maximizing the number of turns, N ; and maximizing the coil factor, k . Each of these factors are constrained by one or more of the following effects:

- (a) magnetic/mechanical stress
- (b) temperature/thermal considerations
- (c) electrical resistance
- (d) high frequency effects, including high frequency resistance and flux trapping.

3.2.2 Stress Constraint Effects

There are many possible toroidal configurations. One of the simplest and most common configurations is a circular toroid as illustrated in Figure 8. The highest magnetic fields in a toroid occur near the major axis or 'core.' It is the core region therefore that produces most of the inductance. Inspection of Figure 8 shows that a circular toroid has only a small region of conductor in the core area. A circular toroid would therefore have a relatively small inductance per unit mass. The high magnetic fields near the core of a toroid also produce high compressive forces in the toroidal windings in the core area. A circular toroid is not well suited to absorbing those loads. Finally, in order to obtain minimum inductor mass the windings must have uniform cross-section. The windings in a circular toroid are in the poloidal direction and in order to achieve uniform cross-section the geometry of the conductor must vary continuously from the core to the outside of the toroid. Circular toroids are therefore not particularly attractive for high current inductive energy stores.

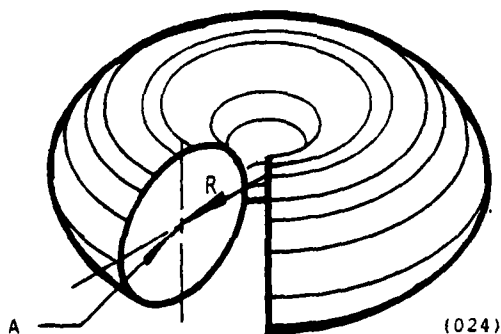


Figure 8. A Circular Toroid.

Many of the problems of circular toroids can be overcome with 'D' shaped windings as illustrated in Figure 9. This configuration puts more of the conductor in the high field region near the core and therefore increases the inductance per unit mass. In addition the highly stressed core region can be fabricated in a more mechanically robust manner. The 'D' shaped toroid however does not address the fabrication difficulties of the circular toroid in that the return conductor along the 'D' must have a continuously varying shape.

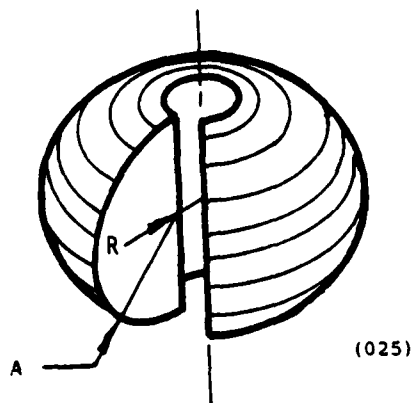


Figure 9. A D-Shaped Toroid.

A third toroidal configuration is illustrated in Figure 10. This configuration, like the 'D' shaped toroid, places a substantial amount of conductor in the high field core region. The core is well suited to taking the high compressive loads. We conclude that D-shaped and rectangular toroids are better suited than circular toroids for low mass, high energy inductors for two reasons: (1) they have a higher inductance per unit mass and (2) the core, which is the region of highest stress in all toroids, is better suited to support the compressive forces.

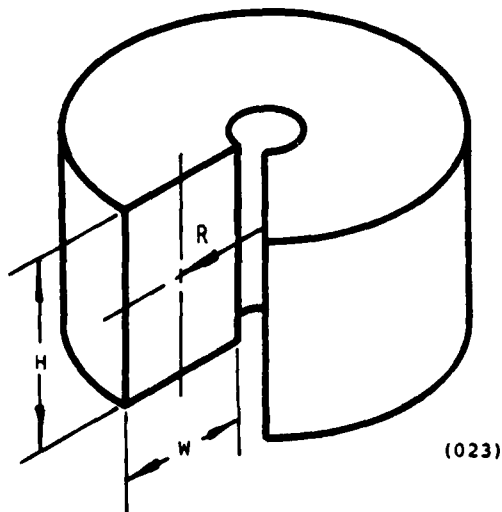


Figure 10. A Rectangular Toroid

3.2.3 Thermal Constraints

We are considering a mode of operation in which the coil is energized to a specified average current level. During that period the coil may be completely or partially discharged many times. It is recharged after each discharge such that the average current level is maintained.

During the pulse the coil conductors dissipate energy and that energy appears as thermal energy in the conductors. There are two choices for handling this thermal energy. The first choice, referred to as thermal inertia, is simply to allow the conductor temperature to rise. A maximum desired temperature increase is chosen and the conductor minimum cross-sectional area can then be calculated. The energy is subsequently removed in the relatively long period between pulses. In the second approach the conductors are actively cooled during the pulse and the conductor temperature remains constant. We have analyzed these two approaches for both coaxial and sectored cores. We found that for pulse times up to 10 s and current levels greater than approximately 10 kA, the thermal inertia approach always resulted in the lightest coil.

3.2.4 Resistance

In some applications coil resistance is an important constraint. The resistance of the core can be readily calculated for either a sectored or coaxial geometry. A thermally constrained core yields the highest core resistance. The resistance may be lowered by increasing the core size. This in turn reduces the thermal problems, but increases the mass and size of the coil. The optimum coil design (i.e., least massive) seldom results in an optimum system. The tradeoff between coil resistance and coil mass can only be evaluated by optimizing the entire system.

3.2.5 High Frequency Constraints

3.2.5.1 High Frequency Effect on Inductance

A well known high frequency effect on impedance is the 'skin effect.' At high frequencies flux penetrates only the outer portion, or skin, of the conductor. The effect is the same as decreasing the cross-sectional area of the conductor and results in the resistance increasing as the frequency of the current increases. The same phenomenon affects the inductance of a

component but in a slightly different manner. While the effect on resistance is caused by flux 'exclusion,' the corresponding effect on inductance is caused by flux 'trapping.' The result of flux trapping is that an increase in frequency causes a decrease in the inductance of the component.

It is important to consider flux trapping when designing a coil because it limits the amount of energy that can be extracted from the coil in a short pulse. Consider that an energy storage coil for pulsed power applications is charged over a long period of time, and then discharged for a time that is relatively short compared to the charging time. Charging over a long period of time can be thought of as low frequency, and discharging in a short time as high frequency. Because the inductance of the store is a function of frequency, the energy that is discharged at high frequency will not be as much as the energy that was stored at low frequency. The energy that is not extracted during the short pulse is 'trapped' in the coil and results in circulating currents that dissipate the energy as heat in the coil conductors.

The energy that is trapped corresponds to the flux in the conductor and the energy that is extracted in a short pulse corresponds to the flux in the 'open' area of the coil. These two regions are depicted in Figure 11. The energy dissipated in the coil is especially important in rep-rated systems. The trapped energy can be minimized by designing 'thin' coils, that is, coils with a winding thickness that is small compared to the coil radius.

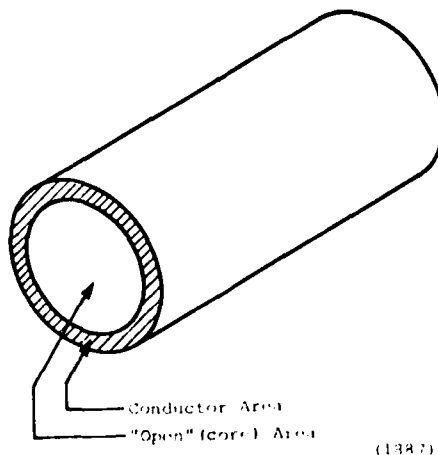


Figure 11. Flux Trapping in a Solenoidal Coil.

Thin coils store a large portion of the energy in the (air) core and store a minimum of energy in coil conductors.

3.2.5.2 High Frequency Effect on Resistance

The other important high frequency effect is the skin effect resistance. During discharge the current is confined to the conductor surfaces and the apparent resistance of the coil increases. This effect results in additional energy dissipation and can affect coil performance in some applications.

SECTION 4

THE DEMONSTRATION COIL

In order to prove the principle of sector toroidal coils, we designed, fabricated, and tested a 10 kA demonstration coil. The design of a 'proof-of-principle' inductor is different from the design of a practical coil. In a practical design, one would design an inductor to have the inductance, resistance, and mass required by the application. The constraints in a 'proof-of-principle' design are determined by the capabilities of the test facilities. In this case, the major constraints were power supply limitations and the size of an available cryostat. The coil was designed so that it could be tested at the Wright-Patterson High Power Laboratory and demonstrate many of the most important coil design constraints. These constraints included thermal, stress, inductance, and resistance.

4.1 DEMONSTRATION COIL PARAMETERS

The demonstration coil was designed to conduct a current of 10,000 A for 10 s. The conductor cross-section was chosen so that during the 10 second pulse, the maximum temperature rise would be 100 K in the smallest core conductors and 50 K in the return conductors. The demonstration coil characteristics are summarized in Table I and the coil concept is illustrated in Figure 12.

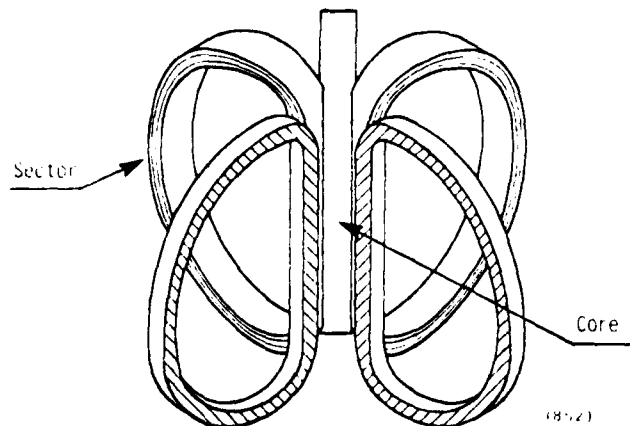


Figure 12. The Demonstration Coil Concept. (The nearest sector is removed to show the coil core.)

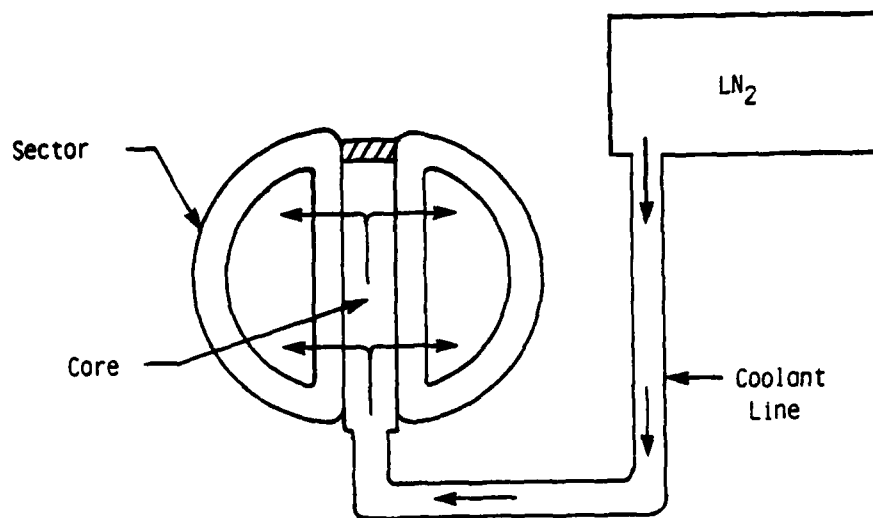
TABLE I
DEMONSTRATION COIL CHARACTERISTICS

Configuration:	Toroidal, sectored
Cross-section:	D-Shaped
Sectors:	6, symmetrically arranged
Turns:	10
Dimensions:	overall height 0.39 m overall diameter 0.47 m
Conductor Material:	Al-1100-O
Interturn Insulation:	Scotchply*
Inductance at 1 kHz:	13.6 μ H
Room Temperature Resistance (dc):	0.93 m Ω
LN ₂ Temperature Resistance (dc):	0.16 m Ω
Rated Current (10 sec. pulse):	10,000 A

* Scotchply is a registered trademark of the 3M Company.
The product is a fiberglass-reinforced, epoxy-resin tape.

4.2 FORCED COOLING SYSTEM

Although the demonstration coil was sized so that active cooling was not necessary, forced-flow cooling was included in the core region so that we could study the performance of a particular cooling system. The forced-flow cooling process consists of three stages: first, liquid nitrogen, the coolant, is supplied to the coil under moderate pressure (less than 20 psi); next the coolant flows into the core of the coil as shown in Figure 13; and finally the liquid nitrogen is directed through coolant passages, and out between adjacent sectors to cool the conductor edges as illustrated in Figure 14. The coolant supply pipe, core region, and coolant channels are visible in Figure 15, a photograph of the partially assembled coil. The complete coil and forced cooling system was designed so that the coil could be operated with or without forced cooling of the core region conductors.



(1550)

Figure 13. Coolant Flow to the Demonstration Coil.

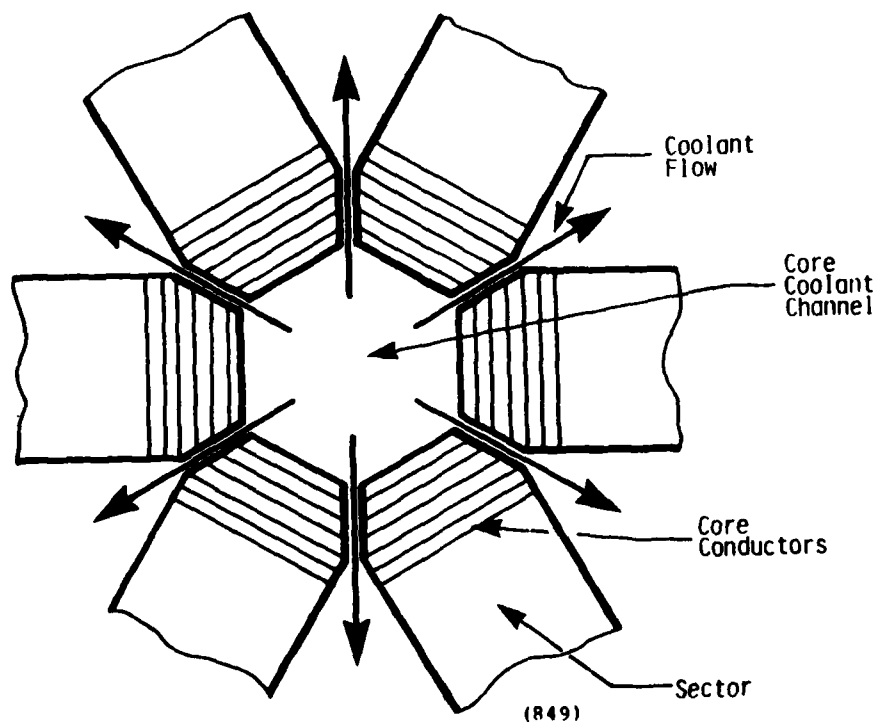


Figure 14. Coolant Flows from the Core Region Out Between Sectors, Cooling the Edges of the Conductors.

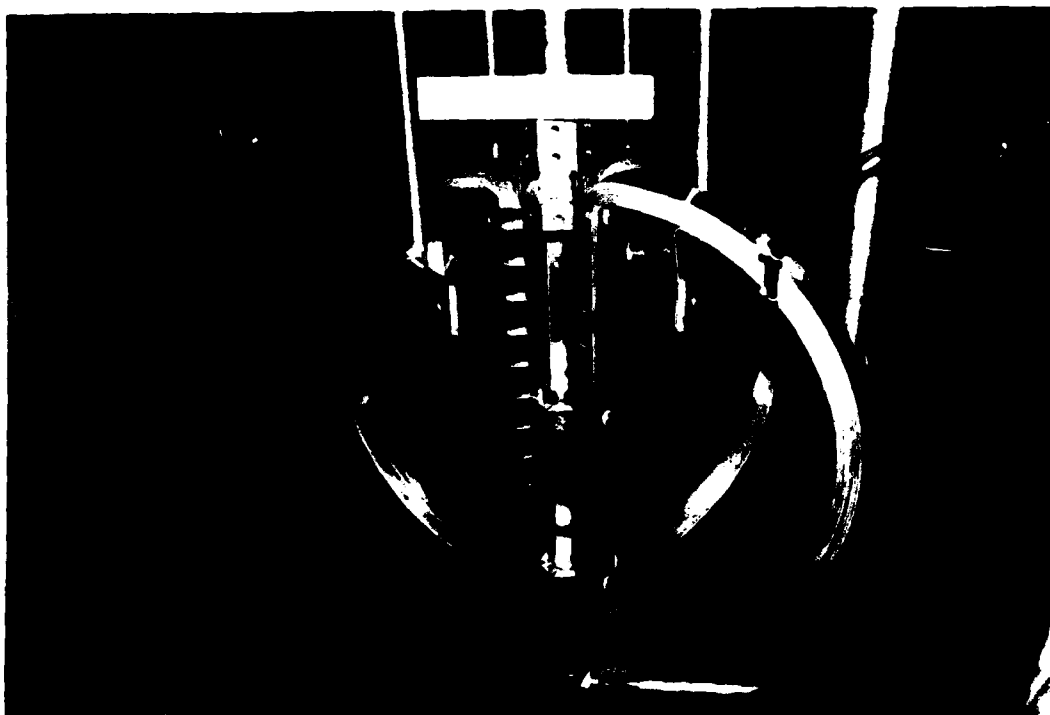


Figure 15. The Coolant Supply Pipe, Core Region, and Coolant Channels are Visible in This View of the Partially Assembled Coil.

4.3 TESTING

The test procedure was organized as four major test series: (1) impedance measurements at room temperature, (2) impedance measurements at cryogenic temperatures, (3) current tests, and (4) active cooling tests. Complete descriptions of the test objectives, procedures, and instrumentation are documented in the Research and Development Test Plan which is appended to this report. The following sections describe the results of the four test series.

4.3.1 Impedance Measurements

The objective of the first two test series was to verify the electrical design of the sectored inductor. To verify the electrical design of the coil, we measured the inductance of the coil components and assembly, and the resistance of the coil components at 78 and 300 K.

4.3.1.1 Inductance

Inductance measurements were taken and analyzed to meet four objectives:

1. To identify damaged or improperly wound sectors.
2. To determine the inductance of the assembled coil and down-leads.
3. To quantify flux coupling between sectors.
4. To measure the amount of flux trapping that might occur at various frequencies.

The results of these four tests are described in the following subsections.

4.3.1.1.1 Sector Inspection. We measured and recorded the inductance of each sector as shown in Table 2. Notice that sectors one and two had a different impedance than the other four sectors. We felt that sectors one and two had turns that were touching or perhaps bridged by small metal cuttings from the machining process. This hypothesis is supported by the value of parallel resistance recorded in Table 2. The smaller magnitude of parallel resistance for sectors one and two indicates an impedance parallel to the sector windings. Windings cannot easily be 'shorted' together in the traditional sense of the word. That is, the resistance of the sector conductor is so small that it is physically impossible to bridge two turns with a resistance that is significantly less than the resistance of the sector. Using impedance measurements to identify improperly wound or damaged sectors we determined that sectors one and two were faulted and that sector six was marginal.

We subjected sectors one, two, and six to a rigorous cleaning and etching process to remove the edges or particles that might be faulting the turns. We measured the impedance of all of the sectors again to evaluate the cleaning process. The final impedance of each sector is shown in Table 3. The recorded values for the impedance of sectors three, four, and five differ from those in Table 2 because, the measurement technique was improved by carefully designing a shielded four-terminal measurement jig. The cleaning process was effective and the final inductance of every sector was within 0.5 per cent of the average sector inductance.

TABLE 2
SERIES AND PARALLEL IMPEDANCE OF COIL SECTORS

SECTOR	Series			Parallel		
	L (mH)	R (ohms)	Q	L (mH)	R (ohms)	Q
1	0.0415	0.078	3.4	0.0477	1.04	3.4
2	0.0412	0.088	3.0	0.0459	0.93	3.2
3	0.0457	0.018	16.2	0.0456	5.26	18.0
4	0.0454	0.018	16.2	0.0456	5.38	18.4
5	0.0453	0.018	16.3	0.0455	5.22	17.9
6	0.0451	0.017	16.7	0.0453	4.65	16.0

TABLE 3
SERIES AND PARALLEL IMPEDANCE OF COIL SECTORS
AFTER CLEANING PROCESS

SECTOR	Series			Parallel		
	L (mH)	R (ohms)	Q	L (mH)	R (ohms)	Q
1	0.0449	0.010	28.0	0.0450	8.1	28.2
2	0.0449	0.010	28.0	0.0450	8.2	28.0
3	0.0451	0.010	29.0	0.0451	8.2	29.0
4	0.0451	0.010	28.0	0.0452	8.2	28.0
5	0.0449	0.010	29.0	0.0450	8.3	28.0
6	0.0448	0.010	29.0	0.0448	8.2	29.0

4.3.1.1.2 Coil Assembly Inductance. We determined the inductance of the assembled coil by measuring the inductance of the assembly and subtracting the inductance of the down-leads. We measured the inductance of the down-leads by replacing each sector in the assembly with a small shorting strip and measuring the inductance of the shorted downleads. The positioned shorting strips are visible in Figure 16. After correcting for test-lead inductance, the assembled coil inductances were:

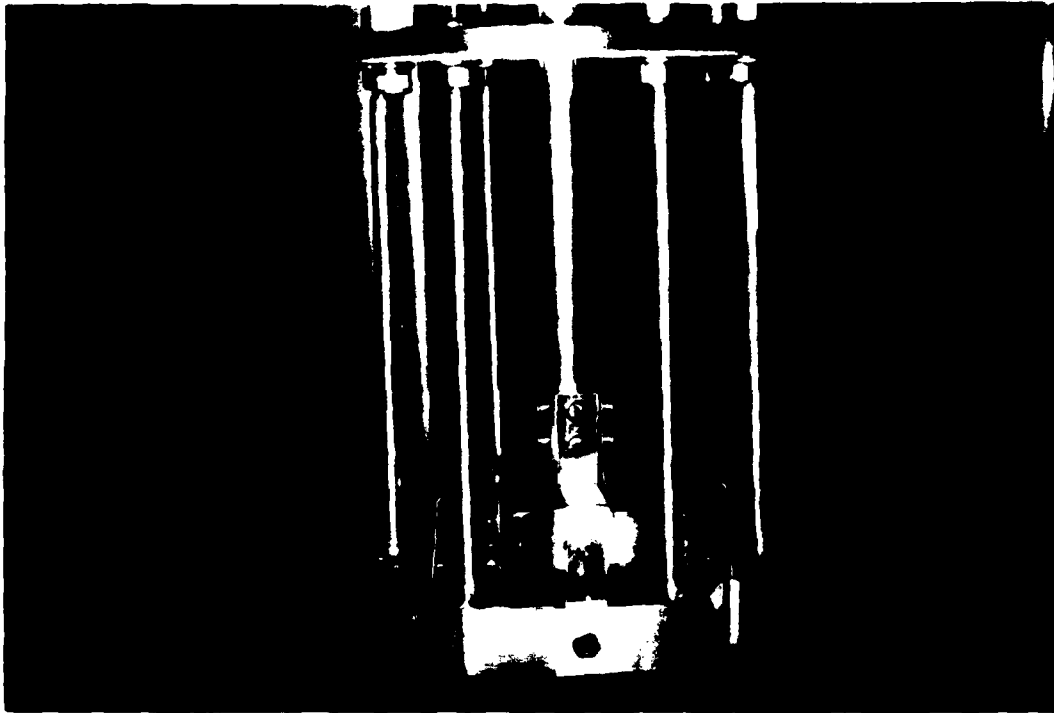


Figure 16. Shorting Strips Replace the Coil Sectors During a Down-Lead Impedance Measurement.

Inductance of Assembly: 0.0139 mH

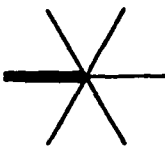
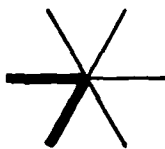
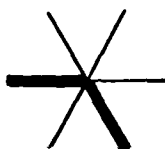
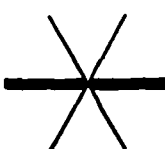
Inductance of Down-leads: 0.0003 mH

Coil Inductance: 0.0136 mH

4.3.1.1.3 Flux Coupling. To quantify the flux coupling between sectors in a sectored inductor, the coil was assembled with various numbers of sectors in several arrangements. The inductance of each arrangement was measured and recorded with a sketch indicating the relative position of the sectors. The inductance of several arrangements is shown in Table 4.

Each arrangement is simply a connection of several inductors in parallel and the mutual inductance between the inductors as shown in Figure 17. Since the value of each inductance is known, and the inductance of the arrangement is known, it is straightforward to calculate the values of the unknown mutual inductances. The coupling coefficient follows directly from the mutual inductance. By comparing the coupling coefficient versus the

TABLE 4
INDUCTANCE OF PARTIAL COIL ASSEMBLIES

CONFIGURATION	INDUCTANCE
	45.1 μH
	28.4 μH
	25.1 μH
	24.5 μH

(1889)

positions of the sectors relative to each other, one can get a much better idea of the effect of the number of sectors on the final inductance of the assembly. A comparison of the coupling coefficient versus relative position of two sectors is presented in Figure 18.

4.3.1.1.4 Flux Trapping. Flux trapping in inductors is characterized by a change in inductance with change in frequency. The significance of this frequency effect was discussed in Subsection 3.2.5.1. To quantify the degree of flux trapping that might occur in the coil, we measured the inductance of the assembly and down-leads at various frequencies. The inductance versus frequency for the coil components is shown in Figure 19.

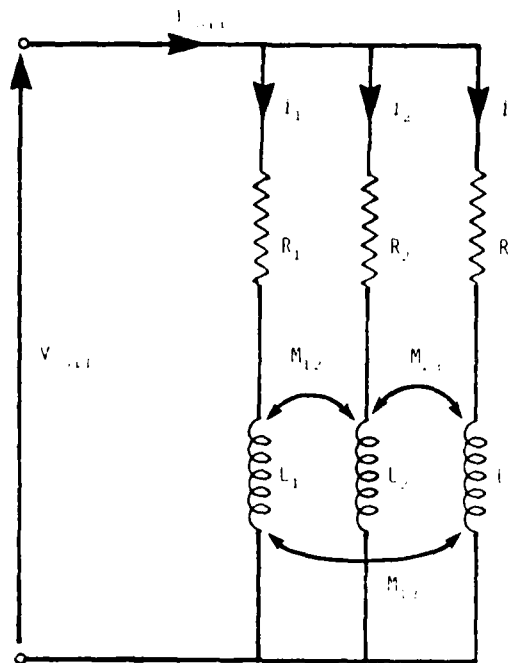


Figure 17. Three Mutually Coupled Inductors in Parallel.

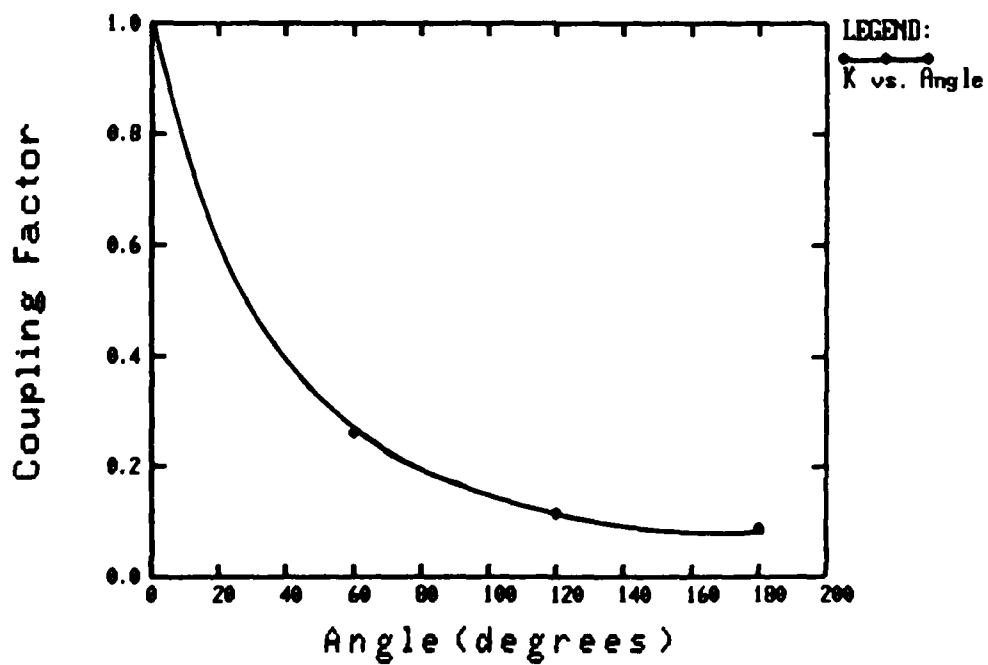


Figure 18. The Coupling Coefficient Versus Angle Between Two Sectors.

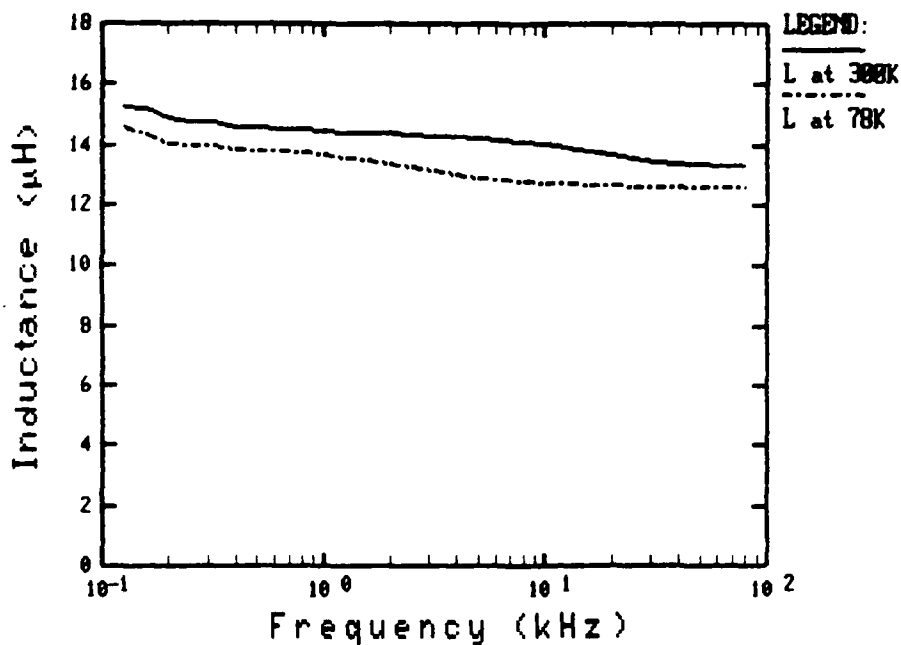


Figure 19. Inductance of the Coil Components Versus Frequency.

Figure 19 can be used to determine how fast energy can be extracted from the coil. For example, the inductance decreases approximately 5% as the frequency is increased to 10 kHz. This indicates that 95% of the stored energy can be extracted from the coil in 25 μ s. The remaining 5% of the stored energy would be dissipated as heat in the coil conductor. It is important in pulsed, and especially rep-rated, applications to account for the difference between energy stored and energy extracted during each cycle.

4.3.1.2 Resistance

The resistivity of pure aluminum decreases by a factor of seven times when it is cooled from room temperature (300 K) to boiling nitrogen temperature (78 K). To verify this change of resistivity for commercially available aluminum, a sample of the 1100-0 Aluminum used to wind the coils was sent to Professor Jim Ho at Wichita State University. Professor Ho measured the resistivity of the aluminum at room temperature and at boiling nitrogen temperature. His resistivity measurements are shown in Table 5.

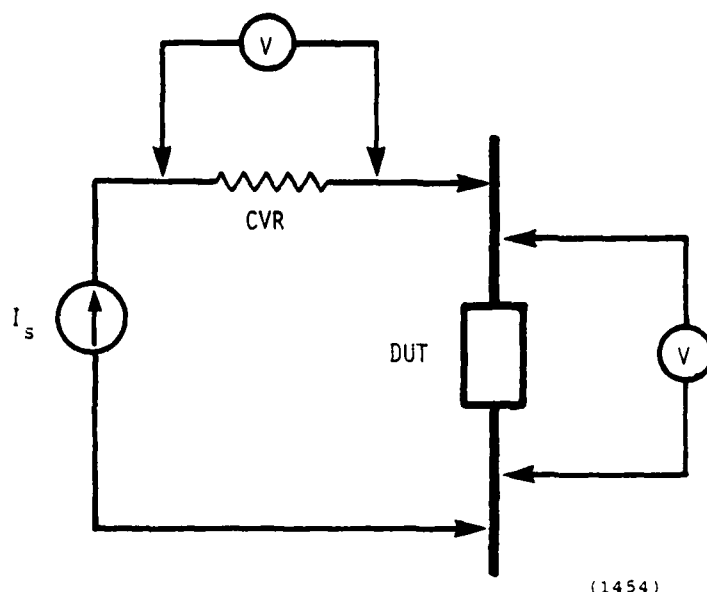
TABLE 5
RESISTIVITY OF 1100-0 ALUMINUM
AT ROOM TEMPERATURE AND BOILING NITROGEN TEMPERATURE

Material	Resistivity ($\mu\Omega$ -cm)		$\rho(298 \text{ K})/\rho(78 \text{ K})$
	298 K	78 K	
Al 1100-0	2.97	0.438	6.78

We measured the resistance of a single coil sector, the down-leads, and the entire coil assembly at two temperatures: 300 K and 78 K. The resistances and calculations of the resistivity ratios are shown in Table 6. We used a four-terminal shunt technique as shown in Figure 20 to make dc resistance measurements accurate to 2%.

TABLE 6
IMPEDANCE OF THE PULSED ENERGY STORAGE COIL
AT ROOM TEMPERATURE AND BOILING NITROGEN TEMPERATURE

Component	Inductance (μH)	Resistance ($\text{m}\Omega$)		Resistivity Ratio
		(300 K)	(78 K)	
One Sector	44.9	5.84	0.855	6.8
Down-leads	0.5	0.207	0.121	1.7
Assembly	14.1	1.14	0.276	4.1
Coil (Assembly - Down-leads)	13.6	0.933	0.155	6.0



(1454)

Figure 20. A Four-Terminal Measurement Technique.

We were concerned that winding the aluminum into a coil and machining the edges might 'work-harden' the material. Work hardening usually results in a slight increase in the resistivity of the aluminum. This effect would be more pronounced at decreased temperatures (less than 80 K) and could be detected by comparing the resistivity ratio of an unworked piece to a piece in which work hardening was suspected. The resistivity ratio in Table 5 represents an unworked piece of aluminum. The ratio for a single sector in Table 6 represents a possibly work-hardened piece. Comparing the two values, 6.78 and 6.8, we determined that any work hardening that may have occurred did not affect the resistivity of the material at 78 K.

4.3.2 Current Tests

Testing the ability of the coil to conduct current in the kiloampere range was done at the High Power Laboratory at Wright Patterson Air Force Base. The current tests were divided into two series: resistance characteristics at the coil terminals, and current sharing between sectors.

4.3.2.1 Terminal Characteristics -- Resistance

The minimum-mass design of an inductor is either stress or thermally constrained. The demonstration coil was thermally constrained to a maximum

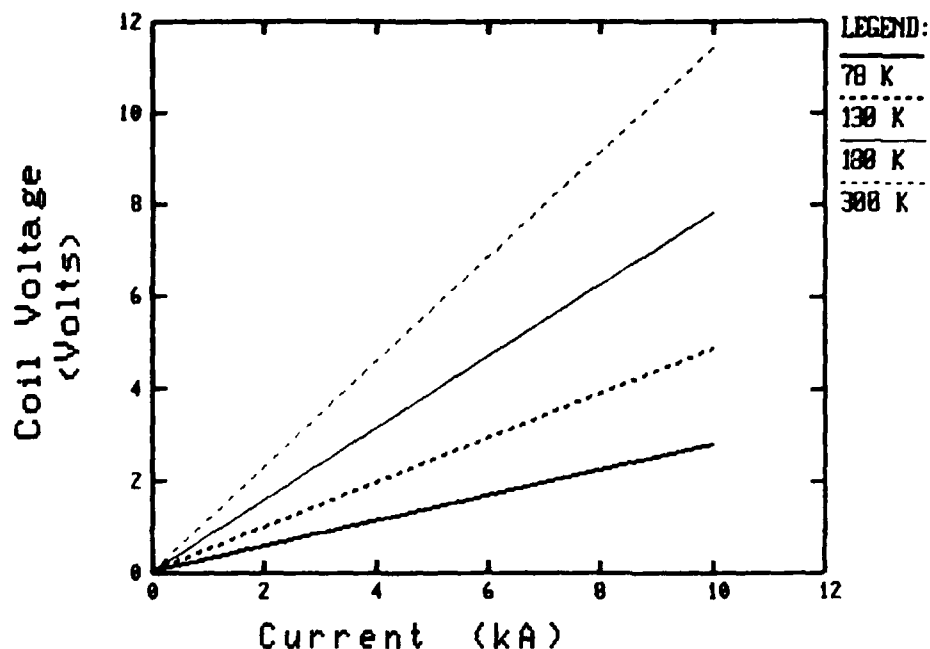
current of 10,000 A. Maximum conduction time was limited by the rate at which the coil could dissipate heat to the surrounding liquid nitrogen bath. Unfortunately, heat transfer rates from conductors to a boiling nitrogen bath are dependent on rather nebulous factors such as surface finish and orientation of the conductors. Calculating the heat transfer rate is further complicated by the fact that most experimental data has been taken for materials such as polished gold. Recording the temperature rise in the aluminum coil conductors of the demonstration coil would yield a better understanding of the thermodynamic properties of practical pancake coils and hence sectored coils cooled by liquid nitrogen.

Measuring the temperature change of the conductors at 78 K with thermocouples would involve measuring millivolt signals from thermocouples to an accuracy of about 10 microvolts. This is difficult to accomplish when the conductor is carrying several kiloamperes and its potential is floating off ground by up to 400 volts.

An alternative method to measuring the temperature of the coil conductors was to measure the coil voltage and current versus time and calculate the coil resistance. The resistivity of the coil conductors is a strong function of temperature, so the temperature could be calculated from the resistance of the coil.

To evaluate the change in resistance of the coil versus time, we need to make current and voltage measurements with little or no drift over periods of tens of seconds. We installed two isolation amplifiers so that the coil voltage could be measured directly and the current could be monitored by measuring the voltage across an existing current viewing shunt. The isolation amplifiers allowed us to make an accurate calculation of the coil resistance as a function of time for any current pulse.

The lines in Figure 21 represent curves of constant resistance. They were calculated based on the measured resistance of the coil at 78 and 300 K. The two curves at 130 and 180 K are estimated by interpolating the change in resistance of the coil parts from the resistances measured at 78 and 300 K. Any increase in temperature during a pulse at a given current would correspond to points above the lower (78 K) curve.



(1552)

Figure 21. Coil Voltage Versus Current at Constant Resistance.

The coil was charged to various currents for various pulse times. The initial and final resistances for these pulses is displayed in Table 7. The maximum current-time product (i^2t) was limited by power supply control difficulties. The LING power supply at the testing laboratory cannot regulate into a very low impedance load such as the demonstration coil. Limited operation was achieved by placing a large magnet in series with the demonstration coil. Unfortunately, the large magnet was designed to conduct 10 kA for only fractions of a second. We were not able to test at higher current-time products during the coil test program.

We were not able to detect a significant increase in resistance during any of the tests. Tests at higher current-time products could yield invaluable data for designers of future high current sector coils. We believe that the procedure described in this section for measuring the coil temperature can be used in future tests to produce much of this data.

4.3.2.2 Current Sharing

An N-sectored coil is a parallel arrangement of N inductances each in series with a small resistance. Additionally, each sector is coupled by a

TABLE 7
COIL RESISTANCE FOR VARIOUS CURRENT PULSES

PEAK CURRENT (kA)	PULSE DURATION (sec)	INITIAL RESISTANCE (mΩ)	FINAL RESISTANCE (mΩ)
1.7	4.0	0.25	0.22
3.0	4.1	0.23	0.23
4.5	4.5	0.24	0.24
6.0	5.9	0.25	0.26
6.3	5.2	0.24	0.25
7.5	5.5	0.24	0.25
9.2	8.9	0.26	0.24

mutual inductance to each of the other sectors. A schematic of a three-sector coil was shown in Figure 17. A six-sector coil, such as the demonstration coil, has six self-inductances and fifteen mutual-inductances. Each sector was sized assuming that it would conduct one sixth of the total current. This should have been a valid assumption because the sectors are electrically in parallel and so would conduct equal currents if they have equal impedance. The sectors do have approximately equal impedances because each sector was made as nearly identical to the others as possible. If all the sectors were identical, each would have the same resistance and self-inductance. Additionally, the mutual inductances tend to force equal currents between each of the sectors.

To verify that the sectors shared current equally, we measured the sector currents with Rogowski coils and electrical integrators at various coil currents. The sum of the sector currents was also compared to the total coil current as measured by the series shunt as a check of the measurement technique. Current sharing data at various current magnitudes is shown in Table 8.

From the data in Table 8, we see that the each sector conducted close to one sixth of the total coil current. We estimate the error of the

TABLE 8

SECTOR CURRENT AT SEVEN TEST CURRENT LEVELS

	Total Test Current in Coil							Test	Percent
	SECTOR	2KA	3KA	4KA	5KA	6KA	7KA	8KA	Average Difference of Ideal
NORMALIZED SECTOR CURRENTS	1	.161	.171	.171	.161	.161	.161	.161	-3.1
	2	.171	.161	.171	.161	.171	.161	.151	1.0
	3	.161	.181	.181	.181	.181	.181	.177	6.4
	4	.161	.161	.161	.151	.151	.161	.152	-5.3
	5	.171	.171	.161	.161	.161	.171	.171	-1.3
	6	.161	.161	.161	.171	.171	.171	.181	1.3

averaged sector current measurements to be less than 1%. Sector 3 conducted 6.4% more than one sixth and sector 4 conducted 5.3% less than one sixth of the total coil current. These small differences in conducted current are reasonable because no effort was made to insure that each sector was assembled and cleaned exactly the same as the others.

4.3.3 Forced Cooling System

We planned to test the forced convective cooling system at three different flow rates. We would monitor the performance of the forced cooling by calculating the temperature rise in the core conductors as a function of time for each flow rate.

As mentioned in subsection 4.3.2.1, the maximum current-time product at which we were able to test the coil was limited by the power supply and magnet shunt. At the maximum current-time product, 200 MA²s, and no coolant flow, the coil resistance did not change noticeably during the current pulse. A much higher test current and current-time product would be necessary to evaluate the forced cooling system performance.

4.4 EVALUATION

The demonstration coil met or surpassed all design specifications. The coil was conservatively rated at 10,000 A for conduction times up to 10 s. This (conservative) limit was based on thermal heat transfer considerations in the core area. We tested the coil to a maximum of 9200 A for pulses of

up to about 5. During the test period, the operators of the test facility began work to modify the power supply shunt so that the power supply may be operated up to its full rated current of 12 kA with small loads such as the sectorized demonstration coil. It is unfortunate that this work was not completed during this contract period because the coil performed exceptionally well up to the maximum output of the power supply.

Evaluation of several key design issues is discussed in the following sections.

4.4.1 Coil Resistance

The resistance of the coil decreased by a factor of seven as it was cooled from room temperature to boiling nitrogen temperature. The resistivity ratio is the same for an unworked piece of the same aluminum. This indicates that toroidal coils can be wound from commercially pure aluminum using the sectorized coil approach without affecting the benefits of cooling the coil to 78 K. The benefits of cooling are a decreased resistance or higher electrical efficiency and come with the added complexity of cryogenics and associated systems. The system payoff (or loss) would have to be evaluated for each application to determine if cryogenic cooling resulted in a more optimum system. The benefits of cryogenic cooling are negated if the coil cannot be maintained at near cryogenic temperatures during current conduction. The sectorized concept results in a coil that can be conveniently cooled during current conduction.

4.4.2 Current Sharing

Each sector of the demonstration coil conducted within 6.4% of one-sixth of the total coil current. No special measures were made to insure that each coil conducted exactly one-sixth of the total coil current. The high degree of current sharing was expected and occurs due to three factors: (1) the sectors were all constructed on the same mandrel and were thus nearly identical in size and shape, (2) the resistance of each sector is a strong function of temperature and tends to force equal current conduction, and (3) the sectors are inductively coupled to each other making the current sharing especially stable during transient conditions such as coil charging and discharging.

4.4.3 Forced Convective Cooling

The forced convective cooling system was not tested to determine its effectiveness in cooling the coil core area. The system was tested to determine if reasonable coolant flow rates could be generated with moderate pressure on the coolant supply Dewar. We found that we could supply coolant to the core region at 0.5 l/s with 25 psi pressure on the supply Dewar. The coolant supply system performed well and should certainly be considered in place of a cryogenic pump in any laboratory or practical cooling application. The effectiveness of forced convective cooling on the coil performance is important to know and can hopefully be evaluated in future tests of the coil.

SECTION 5

CONCLUSIONS

The sectored toroidal inductor meets most present and future Air Force needs for inductive energy storage and pulse forming. The 10,000-A coil built and tested to demonstrate the sectored-coil concept surpassed all design parameters. Additional performance data will be available as the coil is used in switching studies during the next several years.

Designing and testing the sectored toroidal inductor led to the following conclusions:

1. The coil is simple to construct compared to any other present concept to build practical high current toroidal inductors.
2. The coil is well suited to cryogenic operation because it is easy to immerse in liquid cryogen and can be constructed with materials that are usable in cryogenic environments.
3. The open sectored concept allows a variety of cooling schemes not possible with most other toroidal coil concepts.
4. Electrical insulation can be tailored to meet the application.
5. Fringing fields vary as $1/r^8$ for a six-sector coil, extremely low and well suited for practical applications.
6. The design is rugged and easy to tailor to meet various stress or thermal constraints.
7. The sectored coil could be constructed when scaled to at least several million amperes because the pancake sector concept allows wrapping multiple parallel current conductors.

SECTION 6

RECOMMENDATIONS

The demonstration coil performed exceptionally well to the limit of the existing test facilities. We have carefully reviewed the state of the art in coil design and the demonstration coil program and concluded that two projects be undertaken:

1. The 10,000-A demonstration coil should be tested at higher currents and for longer times. Testing at up to 20,000 A and for periods of 5 to 60 seconds would give data that would be extremely valuable in full scale (>100 kA) coil designs.
2. A full-scale (100-1000 kA) coil should be built and evaluated for use in practical applications. There is no other toroidal coil design that shows such great promise to meet present and future Air Force needs in applications such as airborne or space-based electromagnetic launchers.

APPENDIX A

**Magnetic Fringing Fields Around a
Multisector Toroidal Inductor**

Donald E. Johnson

TABLE OF CONTENTS

Section		Page
1	INTRODUCTION	42
2	FRINGING FIELD ANALYSIS	45
2.1	Theory	45
2.2	Computer Modeling	45
2.3	Description of the Coil Geometry	45
3	RESULTS OF THE FIELD STUDY	47
3.1	The Field in the Coil Midplane	47
3.2	The Field in the Sector Plane	48
3.3	The Field on the Coil Axis	48
3.4	The Field on the Sector Axis	49
4	CONCLUSIONS	51

LIST OF FIGURES

Figure		Page
1	Circular Toroidal Coil	42
2	Rectangular Toroidal Coil	42
3	A Coaxial Toroidal Coil	43
4	Sectored Coaxial Toroidal Coil	44
5	A Four-Sector Filamentary Coaxial Coil	46
6	Magnetic Field Intensity in the Coil Midplane	47
7	The Magnetic Field in the Sector Plane of a 4-Sector Coil	48
8	Magnetic Field Intensity Along the Sector Axis	49

SECTION 1

INTRODUCTION

Minimizing system mass is the top priority in many pulsed power applications. Inductive energy stores are often considered because they have low specific mass and volume characteristics. An attractive configuration for applications requiring inductive energy storage is a toroidal coil. Circular and rectangular toroidal coils are shown in Figures 1 and 2 respectively.

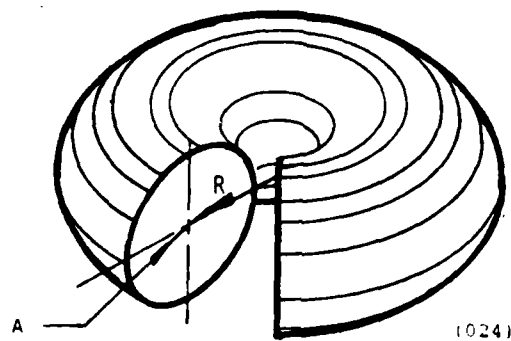


Figure 1. Circular Toroidal Coil.

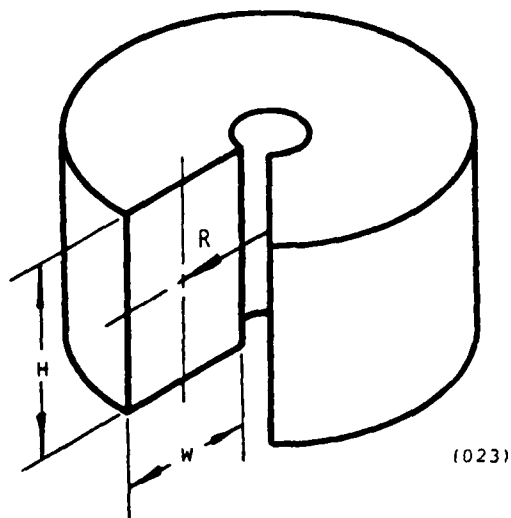


Figure 2. Rectangular Toroidal Coil.

A toroidal coil does not usually store as much energy per unit mass as a solenoid, but it has the advantage of minimal leakage flux. Flux leakage is minimized because the coil conductors completely enclose all of the flux.

The chief disadvantage of toroidal coils is that they are difficult to construct. Construction problems are intensified when multiturn designs are envisioned. One manner in which a toroidal coil might be realized is the 'coaxial' coil geometry shown in Figure 3. The coil is considered coaxial because each turn can be thought of as a section of electrically shorted coaxial cable. The coaxial coil as shown is still difficult to realize physically. Joining of the tubes to the end plates while preserving inter-turn insulation would be nearly impossible. An approach which may solve the construction problem of coaxial toroidal coils while preserving the advantages of low leakage fields is the 'sectored' coaxial coil. This concept is depicted in Figure 4. The symmetrical arrangement of return paths around a central core approximates the closed coaxial toroid and thus preserves the characteristic low value of leakage flux.

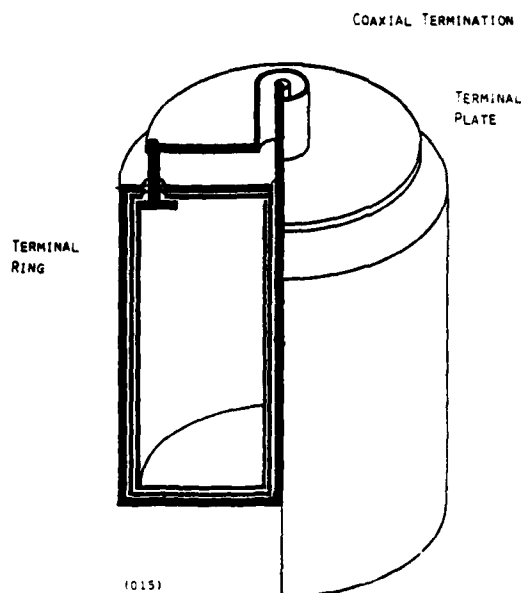


Figure 3. A Coaxial Toroidal Coil.

The magnitude of the leakage fields is inversely proportional to the number of symmetric return paths or 'sectors' used. That is, the more sectors that are used, the better the shielding will be. Unfortunately, the construction is more difficult with higher numbers of sectors. The design problem is then to determine how many sectors provides 'adequate' shielding, and more exactly, how the number of sectors relates to the magnitude of the fringing fields.

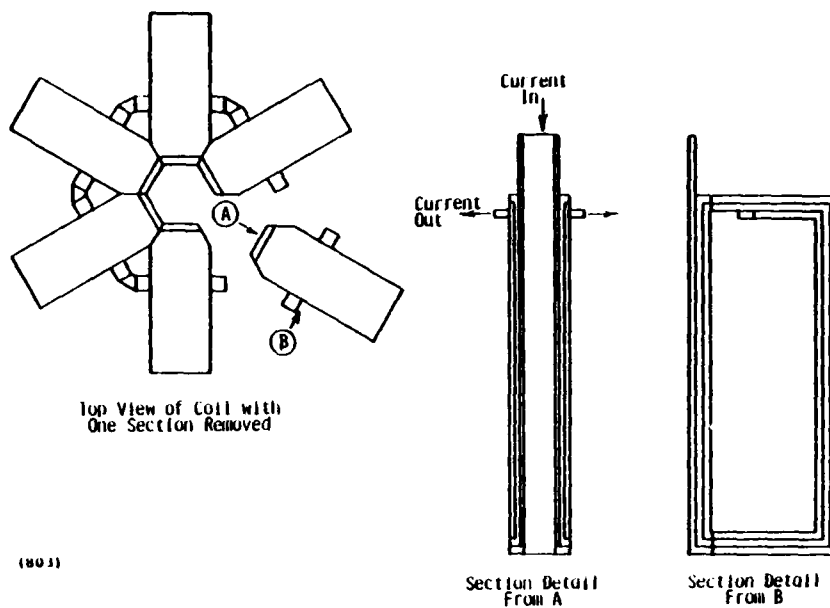


Figure 4. Sectored Coaxial Toroidal Coil

The emphasis of this investigation was to find a relationship between the number of coil sectors and the magnitude of fringing fields. During the study, areas of high and low field magnitude around the coil were defined. These definitions could aid in orienting the coil to avoid interference with sensitive electronic equipment.

SECTION 2

FRINGING FIELD ANALYSIS

2.1 THEORY

The magnetic field that occurs at a point, due to the flow of current in a flat strip, is approximated by current flowing in a linear filament, as long as the point is an appreciable distance away from the conductor. An appreciable distance would be 2 to 3 conductor widths for a strip whose length is much greater than its width. The magnetic field due to a filamentary current, i , of length, dl , can be calculated using the Biot-Savart Law:

$$dB = (\mu_0 i dl \sin \theta) / 4\pi r^2 \quad (1)$$

where B is the magnetic flux density,

μ_0 is the permeability of free space,

θ is the angle between the dl vector and a vector directed from the midpoint of dl to P , the point at which the field is evaluated.

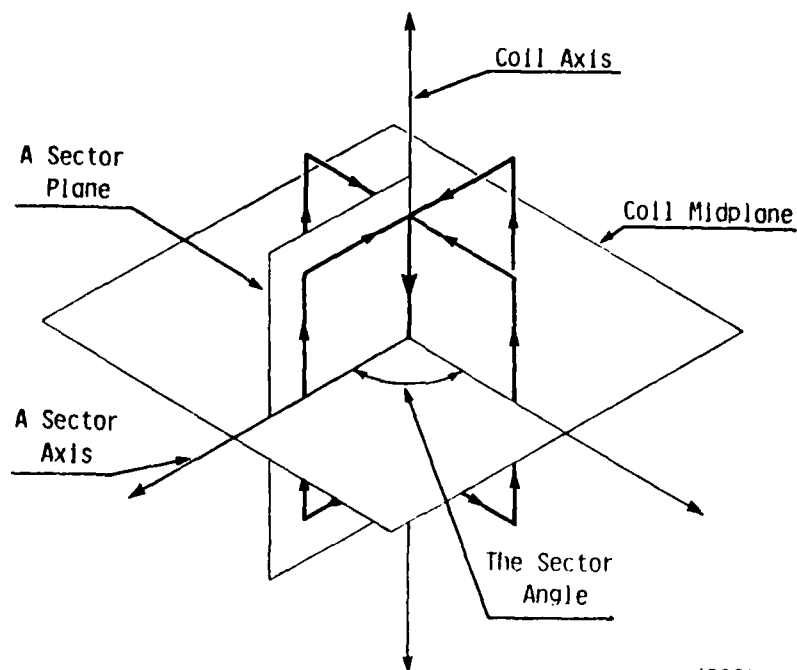
The expression for dB can be integrated to find the field due to a finite length of conductor or a group of such conductors.

2.2 COMPUTER MODELING

We used a digital computer to approximate the integration of equation 1 and evaluated the magnetic field at various points around inductors composed of N_s sectors. A schematic of such a filamentary inductor with 4 sectors ($N_s = 4$) is shown in Figure 5. Regions of high and low field intensity were identified and finally, a curve-fitting routine was used to define the relationship of the magnitude of the field to the number of sectors in the highest field region.

2.3 DESCRIPTION OF THE COIL GEOMETRY

In order to describe the fields around an inductor, it is necessary to define several terms relating to the coil geometry.



(809)

Figure 5. A Four-Sector Filamentary Coaxial Coil.

Referring to Figure 5, the following terms will be used throughout this report:

- coil axis - defined in the usual manner for toroids, as illustrated
- coil midplane - the plane bisecting the toroid and normal to the coil axis
- coil center - the intersection of the coil axis and the coil midplane
- sector - a single section of the coil
- sector plane - the plane of a sector
- sector axis - the axis originating at the coil center and extending along the intersection of the sector plane and the coil midplane
- sector angle - the angle between two adjacent sector axes
- coil radius - a , the dimension of a sector along the sector axis
- nondimensional radius - $r = R/a$, where R is the distance from the coil center to the point of interest.

SECTION 3

RESULTS OF THE FIELD STUDY

The symmetry of the toroidal coil implies that only a portion of the space around a coil need be studied in order to evaluate the field everywhere around the coil. For a sectored coil, the space between two adjacent coils (actually only one half of the space) and on one side of the coil midplane is sufficient. The results can then be repeated for each 'quadrant' and the field will be described everywhere around the coil. The results reported here are organized into four sections, each representing a particular 'zone' of the space around a sectored toroidal coil. The zones are the midplane, the sector plane, the coil axis, and the sector axis.

3.1 THE FIELD IN THE COIL MIDPLANE

The field at a constant radius of 1.2, in the coil midplane, is shown in Figure 6. The horizontal axis is in normalized angle units so that 0 to 1 always represents the sector angle. As would be expected, the field intensity is greatest along the sector axis, or at normalized angles of 0 and 1. This implies that the field can be studied in the sector plane and the field everywhere else assumed to have less magnitude.

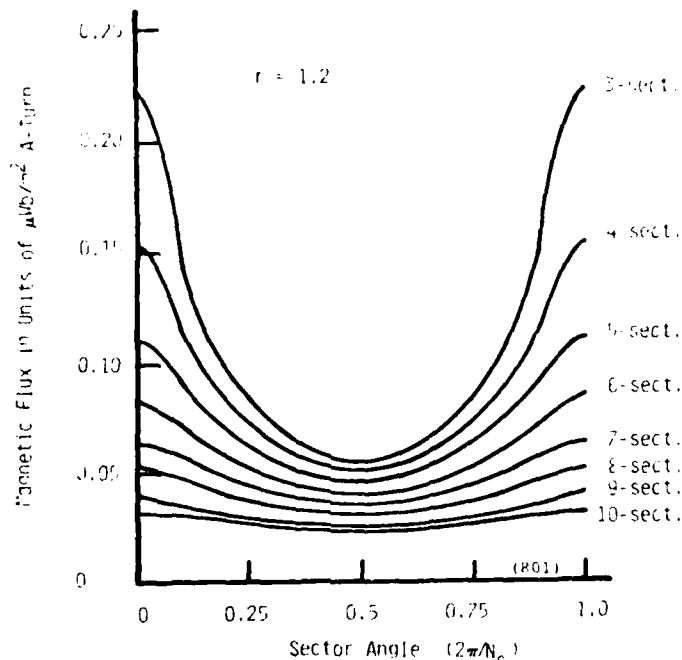


Figure 6. Magnetic Field Intensity in the Coil Midplane.

3.2 THE FIELD IN THE SECTOR PLANE

The field in the sector plane is plotted for constant radii in Figure 7. The angle between the coil midplane and the coil axis is always 90 degrees independent of the number of sectors. The highest value of magnetic field occurs on the sector axis. On a constant radius, the maximum field occurs at 45 degrees, at the 'corner' of the coil. The field is high here because this point is closest to a conductor. The field minimum is always on the coil axis.

3.3 THE FIELD ON THE COIL AXIS

Due to the symmetry of the toroidal coil, the field on the coil axis will always be zero. As shown in Figure 7, there is a cone of approximately 10 degrees from the coil axis where the field is at least an order of magnitude less than the field on the sector axis. This cone describes the best area to place field sensitive equipment which must be placed near the coil.

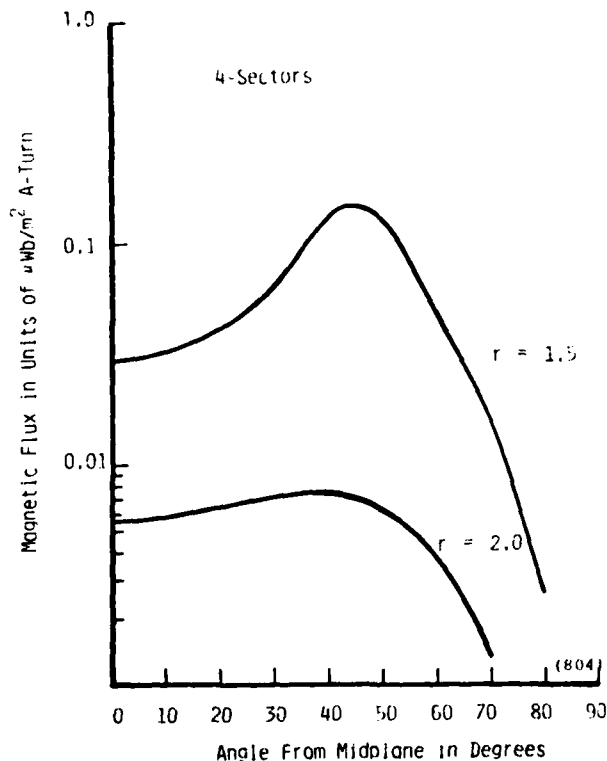


Figure 7. The Magnetic Field in the Sector Plane.

3.4 THE FIELD ON THE SECTOR AXIS

The area of maximum field intensity is along the sector axis. Because this area would be the most troublesome area for nearby components, a detailed relationship was derived for the field in this critical area.

The field intensity along the sector axis decreases as about $1/r^5$. The rate of decrease depends on the number of sectors in the coil. Figure 8 shows the decrease in field intensity with distance for coils of various numbers of sectors. A power curve fit program was used to derive an equation relating the magnitude of the magnetic field to the distance from the center of the coil. The constants of each curve fit relation were then paired with the number of sectors and a curve fit for the two constants was applied. The final result is then an equation relating the magnitude of the magnetic field to the number of sectors and the distance from the center of the coil:

$$B_T = 2.19 \times 10^{-6} N_s^{-0.904} r^{-4.94 \exp(0.0871 N_s)} \quad (2)$$

where N_s is the number of sectors and r is the coil radius.

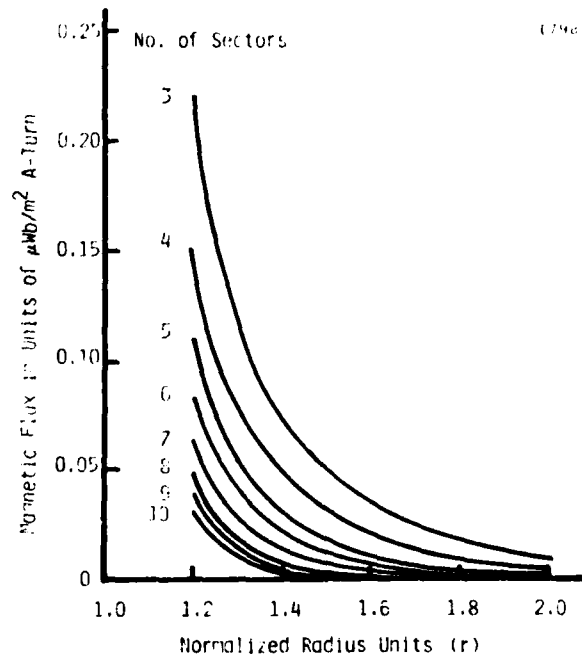


Figure 8. Magnetic Field Intensity Along the Sector Axis.

Equation 2 was derived for an 'optimized' coil geometry, (i.e., one in which the coil height is twice the radius). The total coil current was 1 A and the coil radius was 1 m. The magnetic field intensity is in Wb/m^2 . To apply the equation to other coil sizes and coil currents, it is necessary to multiply the answer by two factors: first, the stored current in the coil in amperes; second, one over a , the radius of the coil in meters.

SECTION 4

CONCLUSIONS

The results of the field analysis in the region surrounding a sectorized toroidal coil led to the following conclusions:

1. The magnitude of the magnetic field is greatest along the sector axis and lowest near the coil axis.
2. The magnitude of the field directly on the coil axis is zero.
3. The magnitude of the fields along the sector axis varies as approximately one over the number of coil sectors. For more than three sectors, this is a relatively weak dependence.
4. The magnitude of the fringing fields along the sector axis decreases as about $1/r^8$ for a six-sector coil.
5. The choice of the number of sectors is highly important only when system design requires that sensitive equipment be placed close to the coil. Orientation of the coil and distance to the sensitive equipment are usually more important design points.

APPENDIX B

**Research and Development Test Plan for the
Pulsed Inductive Energy Store**

**John P. Barber
Donald E. Johnson**

TABLE OF CONTENTS

Section	Page
1 INTRODUCTION	56
2 TEST SERIES 1 - ROOM TEMPERATURE IMPEDANCE MEASUREMENTS. .	56
2.1 Sector Impedance Measurements	56
2.2 Assembly Impedance Measurements	58
3 TEST SERIES 2 - CRYOGENIC TEMPERATURE IMPEDANCE MEASUREMENTS	58
3.1 Sector Resistance at Cryogenic Temperature	58
3.2 Down-Lead Resistance at Cryogenic Temperature	59
3.3 Assembly Resistance at Cryogenic Temperature	59
4 SEQUENCE FOR TEST SERIES 3 AND 4	59
5 TEST SERIES 3 - CURRENT TESTS	61
6 TEST SERIES 4 - ACTIVE COOLING EVALUATION	61
7 RECORDING INSTRUMENTATION	62

LIST OF ILLUSTRATIONS

Figure		Page
1	Time Sequence of Events in Coaxial Coil Test	60
2	Coaxial Coil Test Circuit	61

LIST OF TABLES

Table		Page
1	Test Plan	57

1. INTRODUCTION

This document is a research and development test plan for use on the program 'Pulsed Energy Storage Coil Development and Data' under Air Force Contract No. F33615-82-C-2224. The test plan will be used as a guide in experimentally validating the performance of the Coaxial Inductor under construction on this contract. The test plan defines and describes the various tests and outlines the procedures which will be used in accomplishing these tests.

The test procedure is divided into four major test series: (1) impedance measurements at room temperature, (2) impedance measurements at cryogenic temperatures, (3) current tests, and (4) active cooling tests. Descriptions in terms of test objectives, procedures, data and instrumentation for each of these test series are shown in Table I. The test series are discussed in the following paragraphs.

2. TEST SERIES 1 - ROOM TEMPERATURE IMPEDANCE MEASUREMENTS

The three objectives of these measurements are: (1) to verify the electrical design of the sectored inductor, (2) to identify sectors that might have had turns 'shorted' during winding, and (3) to quantify flux coupling between sectors in coils of various numbers of sectors. The room temperature measurements will be divided into sector measurements and assembly measurements.

2.1 Sector Impedance Measurements

There are several opportunities during the winding and machining of a sector for the turns to become shorted together. These faults can be identified by measuring the impedance of the sector. An inductance reading less than normal would indicate less turns, i.e. 'shorted turns.' It is likely that the fault would also cause a deviation in the normal parallel resistance of the sector. The measurements will be conducted as follows:

- (1) Mark a specific location on a nonmetal bench, at least three feet away from any large metal objects so that each sector is measured in the same way.

TABLE I. TEST PLAN

TEST ISNIES	TEST OBJECTIVES	TEST PROCEDURE	TEST SEQUENCE	DATA TYPE	NUMBER DATA POINTS	DATA DETAILS	SENSORS	RECORDING DEVICES	POTENTIAL PROBLEMS
1-1- PARAMETER MEASUREMENTS IN ROOM TEMPERATURE	Verify electrical design and flux coupling in a selected toroid.	Meas. L and R vs. freq. for each sector, the down leads, and the assembly.	Meas. L and R of L and R vs. freq. Short lead-in. Meas. L and R of lead-in. Meas. L and R of assembly.		One per decade lower avail. freq. of bridge for each component.	L = 0.1-50 μ H. +/- 0.1 μ H. R = 0.05-2 m Ω . +/- 0.1 m Ω . f = DC-100 kHz.	RLC Impedance Bridge	None	Shorted turns, large downlead res., or ind.
1-2- PARAMETER MEASUREMENTS CRYOGENIC TEMPERATURE	Determine the change in resistance with temperature.	Meas. R of a sector, the down leads and the assembly at 78 K.	Meas. R of each sector. Short lead-in. Meas. R of lead-in. Meas. R of assembly.		One for each component.	R = 0.05-2 m Ω . +/- 0.1 m Ω . f = 1 kHz.	RLC Impedance Bridge	None	Work hardening may increase resistivity of aluminum at cryogenic temp.
1-3- CURRENT TEST CRYOGENIC TEMPERATURE	Determine the coil voltage and derive the resistance. Determine current sharing.	Charge coil to rated current.	Charge to 0.2, 0.5, 1.0, 2.5, 5.0, 7.5 and 10.0 kA. Couple volt-ago. thermopile. Cool for not less than 5 min after each test.	Current, voltage, thermopile, couple volt-ago.	Continuous over time from 10 sec before charging to one minute after charging.	1(N) = 50-1700 A Rogowski Coils, Integrators, Voltage Dividers. Vth = 5 mV. I = 0.2-10 kA. (all +/- 5%)		Oscilloscope	Voltage drift, induced voltage on thermocouple leads, poor current sharing.
1-4- ACTIVE COOLING CRYOGENIC TEMPERATURE	Derive heat transfer rate as related to active cooling.	Charge coil and measure voltage and temp. at several coolant flow rates.	Charge to 5.0 kA, meas. V and temp. at 0.5, 1.0, 2.5, 5.0, 7.5, 10.0 kA, and 1.0 liters/sec.	Current, voltage, temp. couple volt-ago, and pressure in coolant down.	Continuous over time from 10 sec before charging to one minute after charging at 3 pressures.	Same as (1). Press. = 0-3 psi +/- 0.5 psi	Same as (1). Pressure gauge on coolant supply down.	Oscilloscope	Same as (1). Pressure may be difficult to regulate on down.

- (2) Fix and mark the position of the bridge and the position of the measuring cable so that it does not move during the test.
- (3) Measure and record the series and parallel impedance of each sector.

2.2 Assembly Impedance Measurements

The room temperature impedance of the toroidal inductor will verify the electrical design of the coil. It will be necessary to separate the impedance of the down-leads from that of the coil. The down-lead impedance will be determined by replacing the coil with a short circuit and measuring the impedance at the assembly terminals. In addition, information about flux coupling in sectorized coils can be obtained by measuring the impedance of the coil with various numbers of sectors in place. The test procedure will be as follows:

- (1) Replace all six sectors with shorting strips.
- (2) Tighten all bolts to insure good electrical connections.
- (3) Record the impedance of the assembly as 'the down-lead impedance.'
- (4) Remove the shorting strips and add sectors in various configurations.
- (5) Record the impedance of each configuration with a sketch that describes the configuration and the serial number of the sector used.
- (6) Attach a shorting strip in place of the assembly.
- (7) Measure the impedance of the test leads attached to the shorting strip.

3. TEST SERIES 2 - CRYOGENIC TEMPERATURE IMPEDANCE MEASUREMENTS

The objective of this test series is to determine the change in resistance with temperature of a single sector, the down-leads, and the assembled toroidal inductor. Test Series 2 is divided into the following three tests:

3.1 Sector Resistance at Cryogenic Temperature

In operation, the sectors are immersed completely in liquid nitrogen. To measure the change in resistance with temperature of a sector, the following procedure will be followed:

- (1) Measure the impedance of the sector at room temperature in the Dewar as it will be positioned during cryogenic measurements.
- (2) Fill the Dewar with liquid nitrogen and allow the sector to cool to liquid nitrogen temperature.
- (3) Measure the impedance of the sector at cryogenic temperature.

3.2 Down-Lead Resistance at Cryogenic Temperature

In operation, the lower portion of the down-leads is immersed in liquid nitrogen, while the upper portion is attached to the power supply current lines. To measure the resistance of the down-leads at cryogenic operating temperatures, the following procedure will be followed:

- (1) Short circuit the down-leads by replacing the sectors with the six shorting strips.
- (2) Install the Dewar header and attach the power supply current lines.
- (3) Measure the resistance of the down-leads at room temperature.
- (4) Fill the Dewar to its lowest operating level and measure the resistance of the down-leads until a steady state resistance is reached.
- (5) Repeat Step 4 with the Dewar filled to its highest operating level.

3.3 Assembly Resistance at Cryogenic Temperature

The following procedure is used to determine the resistance of the coil assembly at cryogenic temperature:

- (1) Assemble the coil and place in the Dewar.
- (2) Attach the power supply current lines to the down-leads.
- (3) Fill the Dewar to its lowest operating level and measure the resistance of the assembly until a steady state resistance is obtained.

4. SEQUENCE FOR TEST SERIES 3 AND 4

The test sequence described in this paragraph will be used with appropriate modifications for test series 3 and 4 involving the AFAPL high current power supply. The important sequencing events in a normal test

sequence involve the power supply, the coolant flow, and instrumentation. A sequence would proceed as follows:

- (1) Check all instruments to assure that deflection factors, calibration, triggering, time bases, etc., are all correctly set.
- (2) Initiate coolant flow.
- (3) Enable instrumentation.
- (4) Verify coolant flow and level.
- (5) Charge the coil with a preprogrammed current pulse.
- (6) Stop coolant flow.
- (7) Deactivate the instruments and collect all data.

The sequence of events, with approximate time scales is illustrated in Figure 1. The coaxial coil test circuit is shown in Figure 2.

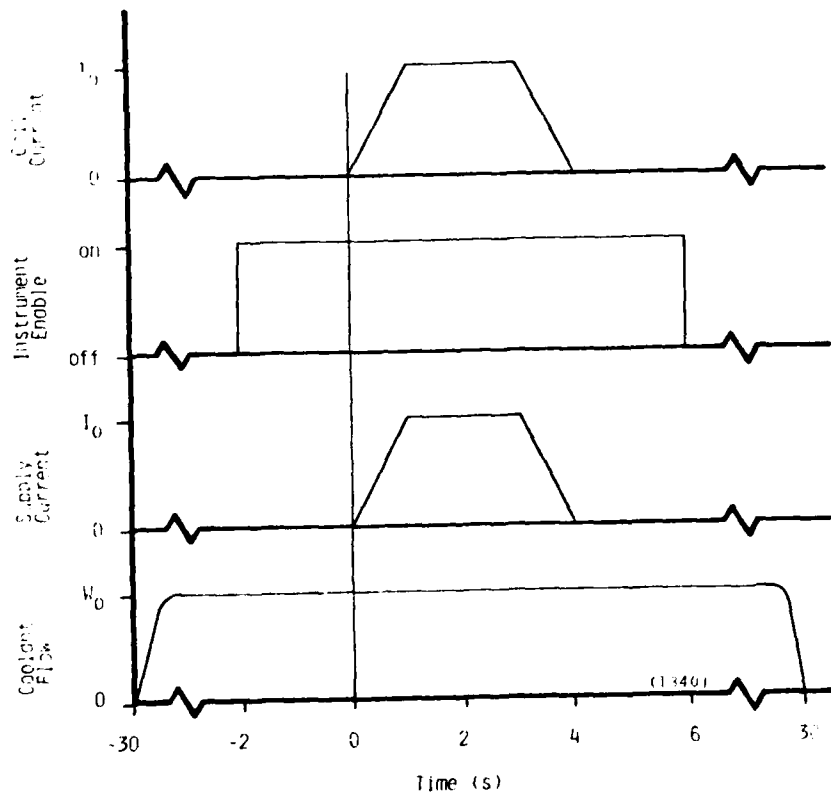


Figure 1. Time Sequence of Events in Coaxial Coil Test.

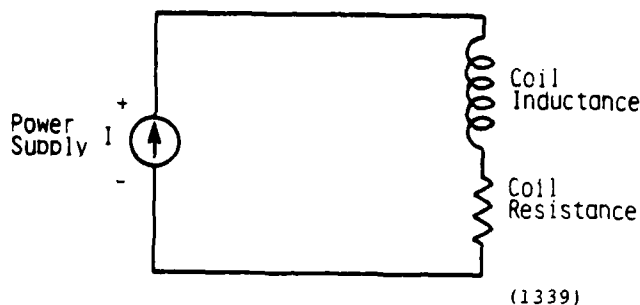


Figure 2. Coaxial Coil Test Circuit.

5. TEST SERIES 3 - CURRENT TESTS

The objectives of the third test series is to verify the current sharing between coil sectors and to measure the terminal voltage of the coil versus current. The coil current will be brought up to rated specifications in several steps.

The sequence described in Section 4 will be followed at the power supply's lowest regulated current and repeated with greater values of current until rated current is achieved. The number of intermediate steps needed will be based on current sharing between sectors and terminal voltage characteristics.

6. TEST SERIES 4 - ACTIVE COOLING EVALUATION TESTS

The objective of the fourth test series is to quantify the degree of active cooling achieved with forced coolant flow in the coil core. A current test at 0, 7.5, and 15 l/s will be conducted at 5000 A. Based on careful analysis of the data gathered in this test series, several sequences may be run for extended times to determine the equilibrium temperature characteristics.

7. RECORDING INSTRUMENTATION

To assure detection of any and all abnormalities during a test a multi-channel continuous recording oscillograph will be used to record all data shown in Table I.

ATE
LME